Individuality across environmental context in *Drosophila melanogaster*

Thomas F. Mathejczyk, Cara Knief, Muhammad A. Haidar, Florian Freitag, Tydings McClary, Mathias F. Wernet* and Gerit A. Linneweber*

Institut für Biologie

Abteilung Neurobiologie

Fachbereich Biologie, Chemie und Pharmazie

Freie Universität Berlin

*: corresponding authors

Contact: mathias.wernet@fu-berlin.de

Gerit.linneweber@fu-berlin.de

Abstract

Over the past decade, several studies have demonstrated that idiosyncratic animal behaviors remain consistent over long time periods. The consistency of individually variable behaviors over time is often referred to as an animal's individuality, or if consisting of multiple traits personality. However, most experimental studies have focused on individuality in a single, well-defined environmental context, whereas it is well-established from population studies that animal behavior is highly context-dependent. The 'person-situation debate' in humans and decades of observations of animal individuality under intrinsically variable natural conditions raise the question of whether and to what extent animal behavior remains stable across different situations, such as changing environmental contexts. For instance, one individual might be generally more visually guided than another, or rely only on one particular visual cue, or even on this very cue only in a specific environmental context. Here, we use a combination of both well-established and novel behavioral assays to demonstrate the relationship between individual behavior and variable environmental context under tightly controlled laboratory conditions in the model system *Drosophila melanogaster*. The consistency of three individual traits (termed exploration, attention, and anxiety) was investigated under changing environmental contexts (temperature, visual cues, arena shape), in both walking and flying flies. We find that individuality is highly context-dependent, but even under the most extreme environmental alterations tested, consistency of behavioral individuality always persisted in at least one of the traits. Furthermore, our quantification reveals a hierarchical order of environmental features influencing individuality. We confirmed this hierarchy using a generalized linear model and a hierarchical linear mixed model. In summary, our work demonstrates that, similar to humans, fly individuality persists across different contexts, and individual differences shape behavior across variable environments, thereby making the underlying developmental and functional mechanisms amenable to genetic dissection.

Introduction

Animal species display enormous interindividual differences in behavior. The temporal consistency of these interindividual differences allows for defining these idiosyncrasies as animal individuality, also called animal temperament, behavioral syndrome, or if the entirety of trait differences between individuals is meant, even animal personality (Andrew Sih et al., 2004; Dall et al., 2004; Gosling, 2008; Reale et al., 2007). Animal individuality has been described for numerous species and behaviors, including: mouse exploration behavior (Freund et al., 2013), great tit feeding preferences (Partridge, 1976), octopus threat responses and feeding behavior (Mather & Anderson, 1993), pea aphid threat responses (Schuett et al., 2011), as well as vinegar fly handedness (Ayroles et al., 2015; Buchanan et al., 2015), olfaction (Honegger et al., 2020), phototaxis (Kain et al., 2012), and object orientation (Linneweber et al., 2020). The temporal consistency of individuality allows for discriminating it from short-term behavioral changes, like internal state variations. Furthermore, temporal consistency of behavior allows modifications by learning (Kahsai & Zars, 2011) and behavior-based natural selection (Lapiedra et al., 2018). Historically, the 'nature vs. nurture' debate (i.e., genome vs. environment) has shaped our understanding of the origins of behavioral individuality (Galton, 1875). Stochastic developmental processes are a more recently found factor (Honegger & de Bivort, 2018; Linneweber et al., 2020), providing an additional layer to gene-environmental interactions (Traynor & Singleton, 2010). Most experimental studies on animal individuality have focused on a single behavior set in a singular environment, yet commonly used definitions of animal individuality in predominantly field-based disciplines such as behavioral ecology (Reale et al., 2007), and the definition of human personality entail behavioral consistency across situations (Mischel, 1968). Similar to humans, animals will never re-encounter the exact same situation under natural conditions, and animal personality can be an important factor in determining the ecological success of an animal and, as a consequence, its entire population (Takola & Schielzeth, 2022). It is, therefore, crucial to understand how an animal's personality or individuality in specific traits interacts with variable environments. Despite decades of interest in animal individuality across situations, the experimental evidence remains

insufficient, and the results are contradictory, with studies arguing for (Briffa et al., 2008; Herborn et al., 2010; Kralj-Fišer et al., 2007; Mowles et al., 2012) and against (Coleman & Wilson, 1998; D'Eath & Burn, 2002) individuality in animals across situations with many finding mixed results (Boissy & Bouissou, 1995; Spoolder et al., 1996; Werkhoven et al., 2021). Here we sought to systematically investigate the consistency of individual behavioral differences across situations using laboratory-controlled variable environmental conditions.

There is ample evidence for the consistency of human personality and animal individuality over time (Costa & McCrae, 1988; Weisbuch et al., 2010). Intuitively, humans attribute consistent personalities to other humans (Ross, 1977). The consistency of human behavior across situations, including environmental context, nevertheless remains highly debated, with several studies arguing for (Costa & McCrae, 1988; Fleeson, 2001) and against it (Hartshorne & May, 1930; Mischel, 1968). Summarized as the 'person-situation debate', psychologists have argued for over a century about the relationship between personality and the situational environment, placing this question at the core of personality psychology (Mischel, 1968). Animal models for behavioral consistency across situations provide an opportunity to address this question. In our study, the situation is the sum of all environmental features where a specific behavioral task is performed. The work presented here establishes a quantitative animal model to investigate this and related questions about behavioral consistency across environmental situations.

The vinegar fly *Drosophila melanogaster* provides an enormous toolset for studying individuality and its origins across multiple scales, from neurons to circuits, to behavior. This comprises a rapidly unfolding connectome (Dorkenwald et al., 2024; Xu et al., 2020; Zheng et al., 2018), an extensive collection of cell type-specific, binary expression systems (Luan, Peabody, et al., 2006; Pfeiffer et al., 2010), and a similarly extensive collection of tools for manipulating neuronal function, including neuronal silencers (Baines et al., 2001; Sweeney et al., 1995), activators (Luan, Lemon, et al., 2006), and thermogenetic (Hamada et al., 2008) and optogenetic (Klapoetke et al., 2014; Pulver et al., 2009) effectors. Hence, the availability of tools and reagents for manipulating small, defined sets of neurons is no longer a major

limitation in answering questions about individual behavioral differences. Instead, what has been missing is an integrative approach combining different high-throughput behavioral assays, which would allow for behavioral screening and classification of large quantities of individual flies for several different behavioral parameters across a variety of environmental contexts.

In recent years, mainly low-throughput, single-fly visual assays like the classical two-stripe Buridan assay (Bülthoff et al., 1982; Götz, 1980), arenas for tethered walking (Seelig et al., 2010) or virtual flight (Mathejczyk & Wernet, 2020) have been used to study behavioral individuality in vison-based tasks (Linneweber et al., 2020; Mathejczyk & Wernet, 2019). In Buridan's paradigm, flies walk between two inaccessible visual targets (two vertical high-contrast stripes). The stripes are presented in a homogenously illuminated surrounding with no other visual or non-visual cues. Apart from work on individuality involving Dorsal Cluster Neurons (DCNs) (Hassan et al., 2000), also known as Lobula Columnar Neuron 14 (LC14) (Otsuna & Ito, 2006), Buridan's paradigm has been used to show the importance of the central complex for normal walking speed (Strauss et al., 1992) and for studying photoreceptor function or development (Kiral et al., 2020; Strauss et al., 2001), and visual memory (Neuser et al., 2008). Other circular arenas have been frequently used to study locomotory activity without visual stimuli (Branson et al., 2009; Robie et al., 2017; Valente et al., 2007).

In contrast to these low throughput assays, high throughput assays for studying the behavioral responses of large amounts of animals have been used primarily for genetic screens. Examples include apparatuses to study phototaxis (Hirsch & Boudreau, 1958), geotaxis (Hirsch, 1959), olfactory learning (Jiang et al., 2016; Quinn et al., 1974), and circadian rhythms (Konopka & Benzer, 1971). The Ethoscope (Geissmann et al., 2017) and MARGO (Werkhoven et al., 2019) are recent additions to this repertoire that offer several additional high-throughput assays. Except for the *Drosophila* activity monitors (DAM, Trikinetiks), Ethoscope, and MARGO, these group assays cannot distinguish individual behavioral differences. Only the Ethoscope and MARGO provide some visual modules. Hence, progress towards understanding individuality in visually guided behaviors in a high-throughput fashion

remains meager, with few exceptions (Ayroles et al., 2015; Buchanan et al., 2015; Kain et al., 2012).

To investigate the influence of the environment on the consistency of visually guided individuality and, to systematically quantify individuality across many behavioral traits and their dependency on the environment in walking flies, we built a new multi-parameter assay called Indytrax. Indytrax is a compact and affordable Mathworks MATLAB-based modular assay and tracker for high-throughput individual ethological quantification. The assay includes swappable modules for multiple high-throughput Buridan paradigms, a Y-maze choice assay for studying the decision-making and locomotor handedness (Buchanan et al., 2015), and a simple setup to quantify locomotor activity in large groups of flies (Branson et al., 2009). We used this tracker to determine the relative contribution of various environmental features (temperature, visual cues, arena shape) to the consistency of individual behavior. Our results show that identically defined visual stimuli (stripe color, width, and length) do not necessarily evoke the same behavior in an individual when presented in different environments. Conversely, we find that specific individual behavioral traits (attention, exploration, and anxiety, categorized via multiple behavioral parameters) remain stable even in different environments. Finally, using an LED-based virtual flight arena, we show that attention towards a stimulus remains stable even across different modalities of locomotion (walking versus flying) when using the same Buridan-type visual stimulus. Hence, we find stable behavioral traits across situations in our fly model, in analogy to what has been demonstrated for humans (Costa & McCrae, 1988; Fleeson, 2001). Altogether, our results provide the foundation for understanding the complex interaction between individuality and the environment, including the question of why individual behavior is more unpredictable in variable naturalistic conditions, much like the consistency across situations in human subjects (Mischel, 1968).

Materials and Methods

Assay and fly number overview

We tested flies across three main behavioral assays and systematically altered five environmental context parameters, but not all flies could be subjected to all environmental context modifications. In the “classical” Buridan assay, we tested 60 flies over three days, 57 different flies with three different stripe numbers, and 54 different flies with three different background illuminations. In the high-throughput assay, we tested 400 flies, with each fly tested in two different temperatures, with light on/off, and in two different arena shapes. In the flight simulator, we tested 30 flies, with each fly tested across two days and three contrast conditions. Furthermore, we tested with 73 different flies in the flight simulator first and then in the “classical” Buridan assay.

Animals

All experiments were performed using one week old wild-type *Drosophila melanogaster* (CantonS (Source: Bassem Hassan) and TopBanana (Warren et al., 2018)) reared on a standard *Drosophila* yeast cornmeal medium (7.5g Agar, 64g cornmeal, 160g yeast, 85.5ml sugar cane syrup in 1L of water) at 25°C and 50% relative humidity under a 12/12 light/dark rhythm. Individual flies were placed into the behavioral arenas using a fine brush and were allowed to accommodate for about 10 minutes before any experiment. The behavioral arenas and flies were cooled on ice for Y-maze experiments before gently loading single flies into the chambers using a fine brush. For experiments with clipped wings, the wings were clipped close to the hinge under CO_2 anesthesia, and flies were tested after being allowed to recover within individual vials for at least two days.

Setups

Setup 1: Standard Buridan Arena

Assay

188 Two Buridan setups were used: type A uses fluorescent tubes for background
189 illumination (as described in (Colomb et al., 2012; Linneweber et al., 2020)). Type B utilizes a
190 panoramical LED matrix (RGB, 384x128 pixels, pixel size 0.9°, 120Hz frame rate, 5kHz refresh
191 rate, < 1ms Pixel update latency), which is easily addressable via HDMI for stimulus
192 presentation (see Fig. 1a). For a detailed description of the assays and tracking procedures,
193 see supplemental Fig. S1. Flies were walking on a circular platform (diameter 12cm) between
194 two opposing black vertical stripes (angular extent 12° horizontal and 90° vertical measured
195 from the center of the platform). A trench of water surrounded the platform to prevent the flies
196 from escaping (type A) or a clear plastic hemispherical dome coated with Sigmacote (Sigma-
197 Aldrich, SL2-25ML) from the inside (type B). Single-fly walking behavior was recorded at 25°C
198 and 50% relative humidity for 15 minutes (450x450, 8-bit greyscale, 20 Hz, AVI, Mjpeg
199 compression, 90% quality). Before changing an experimental condition, flies were placed back
200 into single vials for recovery.

201

202 Automated tracking procedure

203 Data was analyzed either in real-time using previously described code (type A, see
204 (Colomb et al., 2012)) or offline using a custom-written MATLAB code (type B, available for
205 download from github.com/LinneweberLab/Mathejczyk_2024_eLife_Individuality, see
206 supplemental Fig. S1c), respectively. Thresholded video frames and overlaying trajectories
207 are displayed continuously in a separate window to allow the experimenter to assess tracking
208 quality. The MATLAB code works as follows: the circular region of interest (ROI) is
209 automatically detected based on adaptive thresholding and subsequent filtering of the
210 thresholded ROI based on area. Once the ROI is detected, a background image is generated
211 by calculating the maximum intensity between a recorded video's first and last frames. All flies
212 that moved between those frames will not appear in this background-only image. During
213 tracking, the background image is subtracted from each consecutive frame to simplify the
214 thresholding of the fly. For each frame, the centroid of these thresholded pixels is stored.
215 Should more than one object be detected within a ROI (e.g., through pixel noise), the x-/y-

coordinates of the object closest to the fly's position in the previous frame are stored. If a fly is lost, the tracker keeps the last known position of the fly until it is detected again.

Data output

Once tracking is completed, the raw tracking results are converted to real-world units (mm) and saved into a .mat-file. Before further analysis, minimal movements are filtered out by only updating the fly's position if a certain walking threshold (0.8mm/frame) is detected. For each fly, a figure can be saved, allowing for a quick overview of the walking trajectory, and a variety of behavioral parameters are also saved into a separate .txt-file to simplify further data analysis. For a detailed explanation of calculated parameters, see supplemental table 1. For an in-depth analysis of Buridan data, sophisticated data analysis routines describing many behavioral parameters were previously developed (Colomb et al., 2012). To simplify data integration and compatibility, the raw trajectories can also be saved to a pair of .TXT and .DAT files, which can later be read and analyzed by previously available software (Colomb et al., 2012).

Setup 2: IndyTrax multi-arena platform

Assay

To allow for high-throughput behavioral quantification under various tightly controlled environmental contexts, we designed the novel assay system IndyTrax. In short: single flies are transferred to an array of small behavioral arenas. They are filmed from below against near-infrared (850nm + Lee filters 87C IR-pass filter on camera objective) LED illumination (Fig. 3). Compared to published Buridan assays (Colomb et al., 2012), this allows tracking flies in the absence of visible light, but also has the advantage that flies cannot see the camera lens which might otherwise appear as a high-contrast object from within the arena. The assay was designed to allow for the tracking of flies in various possible arena shapes and numbers. We created three different 3D-printable arena types (supplemental Fig. S4e-g), which can be downloaded from github.com/LinneweberLab/Mathejczyk_2024_eLife_Individuality. For

244 individuality analysis, we used the multi-Buridan and Y-maze arenas. The setup was built from
245 commercially available and 3D-printed parts. For a part list, see the supplemental table 2. All
246 3D-printed parts and behavioral assays were printed on a Prusa i3 mk3 printer using black or
247 white PLA filament (Verbatim 55318) and can be downloaded from
248 github.com/LinneweberLab/Mathejczyk_2024_eLife_Individuality. Similarly, the MATLAB
249 code for tracking and data analysis can be downloaded from there. For detailed instructions
250 on how to install and run the code, see the supplemental information. With a computer running
251 MATLAB already available, we estimate the building cost for a complete, temperature-and
252 humidity-controlled enclosure, including all behavioral assays, at about 3500€.
253
254 Temperature- and humidity-controlled enclosure
255 Behavioral arenas are located within a black, climate-controlled metal enclosure.
256 Temperature and humidity within the enclosure can be regulated using two 3D-printed
257 humidifiers and a heating plate (see supplemental Fig. S4a). Ambient temperature and
258 humidity can be set at any desired value using this configuration and kept stable over a long
259 time (see supplemental Fig. S4c). Since small, enclosed arenas are prone to heat build-up, we
260 placed all temperature- and humidity-sensors within the center arena (arena 13) for Buridan
261 experiments and close to the flies in Y-maze experiments. For Buridan experiments, this limits
262 the number of simultaneously trackable arenas to 24 but allows more accurate climate control
263 within the chambers.
264
265 Small-scale Buridan-stimuli arrays
266 We modified the basic design of previously published behavioral arenas optimized for
267 Buridan object orientation behavior (Colomb et al., 2012) by implementing changes in four
268 major areas to allow for high throughput tracking: Firstly, we reduced the arena diameter to
269 allow for filming an array (5x5) of optically isolated Buridan arenas with only a single camera
270 (Fig. 3). Secondly, flies are walking on circular translucent acrylic plates (49mm diameter)
271 which allows for filming flies from below against infrared back-illumination, hence avoiding

problems with dead angles that would arise when filming cylindrical arrays from above. Thirdly, during experiments, flies are contained on their respective acrylic platform by clear hemispherical plastic domes (Fig. 3b). This removes the necessity of cutting the flies' wings before experiments and saves space by making the water-filled moats of the original design superfluous. Plastic domes were coated with Sigmacote (Sigma-Aldrich, SL2-25ML) from the inside to prevent the flies from sitting on the dome surface. Fourthly, to provide a scalable, homogeneously illuminated white background for optical stimulus presentation, the fluorescent tubes of the original design were replaced with electroluminescent (el-)foil wrapped around translucent acrylic cylinders (Fig. 3b). Such el-foils can be cut to size and have low heat emission. They emit light evenly over the whole surface, minimizing unwanted intensity cues within the arenas. El foils are driven at 2 kHz, thus providing virtually flicker-free white illumination to the flies. For creating the Buridan object orientation stimulus, thin black stripes (12° wide as measured from the arena center) were 3D printed and glued vertically to the inside of the arena walls 180° apart, thereby creating high-contrast objects against a uniform white background (Fig. 3b). Individual arenas were fitted into a 5x5 array. Every other arena within the array was rotated by 90° counter-clockwise to increase the robustness of behavioral readouts by canceling out possible directional artifacts created within the enclosure.

Walking behavior was recorded at 50% relative humidity for 15 minutes (1200x1200 pixel, 8-bit greyscale, 15 Hz, AVI, Mjpeg compression, 90% quality) with either the el-foil-illumination on, in darkness, at 23°C or 32°C, respectively. After being tested in the Buridan assay, the flies were put back into single vials overnight to allow for recovery before testing them in the Y-maze assay the next day around the same time.

Y-maze array

We constructed a modular 3D-printable Y-maze array (144 arenas, 300x300x2mm) based on a previously published design (Werkhoven et al., 2019). The Y-maze plates were placed between two 320x320x3mm borosilicate glass plates. The bottom side of the upper

300 glass plate was coated three times using Sigmacote (Sigma-Aldrich, SL2-25ML) to prevent the
301 flies from walking on the upper plate (Fig. 3c). Directly below the arenas and above the upper
302 glass plate, we placed a layer of white paper (Evercopy premium 80g, Ref. 1902C) for light
303 diffusion and to restrict the view of the flies outside of the arenas. For individuality experiments,
304 we covered the outer arenas with black tape and tracked flies only within 100 arenas located
305 in the center. This made keeping track of individual fly identities easier when switching between
306 the different behavioral assays. Videos of walking flies were recorded at 50% relative humidity
307 for 30 minutes (1200x1200 pixel, 8-bit greyscale, 15 Hz, AVI, Mjpeg compression, 90% quality)
308 under white light illumination, in darkness, at 23°C or 32°C, respectively. For white light
309 illumination, we placed a 30x30cm LED panel (Tween Light 30 x 30 cm LED panel, 4000k,
310 16W) on top of the arenas and temporarily removed the infrared-pass filter from the camera
311 objective. Y-maze experiments were all done consecutively on the same day (light on 23°C,
312 light off 23°C, light on 32°C, light off 32°C).
313
314 Automated tracking procedure
315 We developed a fully-automated MATLAB-based tracking code that allows users to
316 adjust parameters like arena number and size and generates output data for all videos within
317 a user-selectable folder. The code assumes only one fly per region of interest. This saves
318 processing time and increases tracking robustness by not having to match multiple fly identities
319 between frames. Before running the code, the experimenter must create a camera calibration
320 file using the MATLAB camera calibration toolbox (see supplemental information). This allows
321 for more accurate tracking results by correcting lens distortions (supplemental Fig. S4d). If the
322 camera stays immobile, this procedure must be done only once, usually in only a few minutes.
323 As long as the arenas filmed are arranged in rows and columns, the code can handle virtually
324 any shape or number of arenas, making it ideal for tracking flies across different behavioral
325 assays (supplemental Fig. S4e-g). Regions of interest (ROIs) are detected based on adaptive
326 thresholding and subsequent filtering of thresholded ROI-objects based on the area
327 (supplemental Fig. S4e-g, middle). Once the ROIs are detected and sorted, a background-

subtracted image is generated, allowing the user to determine a detection threshold, above which all pixels will be interpreted as foreground objects (supplemental Fig. S4e, third from left). During tracking, background subtraction and object thresholding is performed for each frame, and for each ROI the centroid of the thresholded fly is extracted and saved. Thresholded pixels and trajectories are displayed continuously in a separate window to allow the experimenter to assess tracking quality. If more than one object is detected within a ROI (e.g. through pixel noise), the x-/y-coordinates of the object closest to the fly's position in the previous frame is stored. If a fly is lost, the tracker keeps the last known position of the fly until it is detected again. The average tracking speed for 24 ROIs/flies was about 20hz with MATLAB running on an Intel i5 3Ghz CPU. For tracking 400 ROIs/flies average tracking speed was about 5hz.

Data output

Data output is the same as described for our standard Buridan arenas.

Setup 3: Virtual flight simulator

Assay

We designed a novel, easy-to-assemble, and easy-to-use virtual flight simulator using affordable 3D-printable and off-the-shelf parts (Fig. 5a-c) to quantify behavioral responses during flight. For a detailed description of the setup and custom code, see supplemental Fig. S9. In short, using a tethering station (for description, see (Mathejczyk & Wernet, 2020)), flies were cooled down for immobilization and glued to a steel pin (0.1mm diameter, 10mm length, www.entosphinx.cz) using UV-cured glue (Bondic). Once tethered, single flies were put between two neodymium magnets (magneto-tether; upper magnet: diameter 5mm, lower magnet: ring, outer diameter 10mm, inner diameter 5mm). Once the appropriate distance between the magnet is found (about 20mm), the magnetic field allows the flies to rotate freely around their yaw-axis while keeping the steel pin in place (Fig. 5b). The tip of the steel pin is inserted into a V-shaped sapphire bearing (1mm diameter) to reduce friction. For re-initiation

356 of flight, air puffs can be delivered from below via a membrane pump. A panoramic LED matrix
357 surrounding the magneto-tether was used for Buridan stimulus presentation (RGB, 256x128
358 pixels, 120Hz frame rate, 5kHz refresh rate, pixel size 1.4°, angular extent 360° horizontal x
359 100° vertical, stripe width: 12°). The LED matrix controller is connected to a computer via
360 HDMI, allowing an easy and flexible stimulus creation and presentation (Novastar mctrl 660
361 pro, 120Hz, < 1ms Pixel update latency). Flies were filmed from below under near-infrared
362 illumination (Fig. 5c), and each fly's heading was tracked in real-time (90 Hz) using a custom-
363 written MATLAB code (available for download from
364 github.com/LinneweberLab/Mathejczyk_2024_eLife_Individuality). Before starting the
365 experiment, each fly was tested for 120s with an optomotor stimulus (rotating stripe pattern,
366 120°/s, 40x CW and 40x CCW, respectively) to assess the flies' ability to rotate smoothly (Fig.
367 5d, left). After this, flies were presented with the Buridan stimulus with varying contrast (100%,
368 50%, 100% inverted; stripe width 30°), and their heading was tracked for 3x4 min. Flies were
369 then carefully separated from the steel pin and transferred into single vials for overnight
370 recovery before being re-tethered and tested the following day around the same time. For flight
371 vs. walking experiments, flies were tested for 10 min while flying under a 100% contrast
372 Buridan stimulus (stripe width 12° from a fly's perspective) before being gently separated from
373 the steel pin and being transferred into the LED Buridan assay (Type B), where they were
374 tested for 15min under a 100% contrast Buridan stimulus (stripe width 12° from a fly's
375 perspective).
376
377 Automated tracking procedure
378 The code for tracking a fly's heading in 360° can be downloaded from
379 github.com/LinneweberLab/Mathejczyk_2024_eLife_Individuality. Flight tracking is done in
380 real-time at 90fps (see supplemental Fig. S9c). A timestamp is created for each incoming
381 camera frame, and two different thresholded images are computed with different Gaussian
382 filter settings. A strong filter setting blurs out the legs of the fly and allows for thresholding only
383 the fly's body and calculating a heading angle between 0° and 180° through ellipse fitting. By

subtracting the thresholded body pixels from a weaker filtered version of the same frame, the limbs and wings (visible when the fly stops flying) can also be tracked separately if the experimenter wants. To calculate the heading between 0° and 360°, the centroid of thresholded body pixels is set to (0,0) within a fictive coordinate system (see supplemental Fig. S9c), and the body axis is aligned with the x-axis. The head region is assigned based on the sum of pixels within the 4-axis quadrants (smallest area of either I+IV or II+III, respectively). Once the heading is calculated, it is stored together with the original video frame for additional offline data analysis, if desired. When a fly stops flying (wings get detected in the video), a command is sent to a connected Arduino, which controls a relay to switch on a membrane pump and provide an air puff to reinitiate flight. During tracking, the thresholded video is displayed together with the computed heading to allow the experimenter to assess tracking quality.

Data output

After tracking, raw heading data, a graphical overview image, and a table containing computed behavioral parameters are saved automatically for each fly which can be used for further data analysis. For a detailed explanation of all calculated parameters, see supplemental table 1.

Data and statistical analysis for all experiments

All data analysis was performed with MATLAB. For angular calculations, we used algorithm presented in (Berens, 2009). After a test for normality (Shapiro-Wilk-Test), behavioral data between groups was compared using the paired T-test. For correlating individual data, we calculated Pearson correlation coefficients. For walking data, an arena's center region (edge-corrected area) was defined as the circular area around the center with a radius of 80% of the arena radius. The maximum color value (red) for generating heatmaps was set to the 95%-quantile of the count distribution to increase data visibility. Flies that did not move during the experiment were excluded from the analysis.

412

413 **Generalized Linear Model (GLM)**

414 To summarize and generalize the findings from all experiments in this study (using individual
415 rank differences upon changing one or more environmental parameters), a Generalized Linear
416 Model (GLM) was trained using the environmental parameters as predictors (0 when
417 environmental parameter was not changed and 1 if it was changed for any given experimental
418 group) and the resulting individual rank differences as the response variable. Since the five
419 environmental parameters are not fully statistically independent (e.g., arena and vision were
420 altered only in walking experiments and not in flight), we employed ridge regression to mitigate
421 collinearity among these predictors and to control for overfitting. In contrast to stepwise or
422 LASSO regression, ridge regression allowed us to keep all environmental parameters as part
423 of the model. A range of regularization parameters (λ) was tested using 5-fold cross-validation
424 over a log-spaced grid (10^{-6} - 10^{6}) to identify the optimal value that minimized the mean
425 squared error (MSE). Z-scoring was applied to the predictor variables prior to model fitting for
426 data normalization. To estimate coefficient variability and assess significance, bootstrapping
427 was applied. For each of the 1,000 bootstrap iterations, predictors and response data were
428 resampled with replacement, and the ridge regression model was refit using the optimal λ.
429 Coefficients and intercept values from each bootstrap sample were stored, and their
430 distributions were used to calculate the mean coefficients, standard errors (SEs), and p-values
431 for coefficients based on t-statistics derived from bootstrapped SEs.

432

433 **Hierarchical linear mixed-model**

434 We collected behavioral data from all tested walking and flight assays and summarized the
435 five previously quantified behavioral traits under different environmental contexts for walking
436 and flight behaviors, respectively. For each trait, we fitted a hierarchical linear mixed-effects
437 model in Matlab (using the fit lme function) with environmental context as a fixed effect and fly

438 identity (ID) as a random intercept. Fixed effects were included to account for systematic
439 differences due to the different environmental contexts whenever multiple context levels were
440 tested for that trait. This controls for behavioral population-level shifts caused by changing the
441 day, temperature, visual conditions, or the arena shape. Such a model partitions variance into
442 within-fly and between-fly components. We computed the intraclass correlation coefficient
443 (ICC) from each model as the between-fly variance divided by total variance. ICC, therefore,
444 quantified repeatability across environmental contexts. We estimated 95% confidence intervals
445 (CI) for ICC using non-parametric bootstrapping (flies were resampled with replacement across
446 contexts, and models were refitted 1000 times).

447

448 **Results**

449 The goal of our study was to understand to what extent animal individuality is influenced
450 by situational changes in the environment, i.e., how much of an animal's individuality remains
451 after one or more environmental features change. Based on our previous work on animal
452 individuality (Linneweber et al., 2020), we started our analysis in the multiparametric two-stripe
453 Buridan's paradigm (Fig. 1a, supplemental Fig. S1 for technical details) (Colomb et al., 2012;
454 Linneweber et al., 2020). As expected, we measured interindividually variable, yet remarkably
455 consistent behavioral responses, both on the individual (Fig. 1b, Fig. 2a, supplemental Fig.
456 S3a) and mean group level (average of all individuals in the same situation, supplemental Fig.
457 S2a), when tested in the exact same situation with all environmental features kept the same.
458 This was true for the five representative behavioral parameters (out of 20 parameters total,
459 see supplemental Table T1 and supplemental Fig. S8), defined in three behavioral traits:
460 exploration (% of time walked, walking speed), attention (vector strength, angular velocity),
461 and anxiety (centrophobicity). The exploration trait is characterized by parameters describing
462 activity. Parameters related to attention reflect heightened responses to visual cues, but unlike
463 commonly used metrics such as angle or stripe deviations (Colomb et al., 2012; Linneweber
464 et al., 2020), they can be calculated in the absence of visual cues. Lastly, the parameter
465 centrophobicity, used as an indicator of the trait anxiety, is linked to the open-field test in mice,
466 where the ratio of wall-to-open-field activity is frequently calculated as a measurement of
467 anxiety (Carter & Shieh, 2015).

468 Modifying the visual stimulus within the Buridan arena (0, 1, and 2 stripes were tested,
469 Fig. 1c, Fig. 2b, and supplemental Fig. S2b and S3b) significantly affected the mean group
470 behavior across all three behavioral traits (supplemental Fig. S2b). Especially, the means of
471 the three parameters (% of time walked, vector strength, and centrophobicity) were strongly
472 affected by the stimulus modification. Surprisingly, despite this change in group means, we
473 observed only a minor effect on individuality when testing the same fly in different situations
474 (Fig. 1c and Fig. 2b, measured by a high Pearson correlation coefficient and a consistent rank
475 within the distribution). The individuality for the traits exploration and anxiety persisted even

upon modulation (variation of stripe number) and after removing visual cues from the arena. Only those parameters describing the fly's attention towards visual cues showed an unsurprising reduction in behavioral consistency upon removal of the visual stimuli (Fig. 2b). Altogether, these results demonstrate that individuality persisted after stimulus modifications within the same arena, even when the modifications resulted in altered group responses.

To further characterize the surprising relationship between individuality and group means upon situational changes, we modified the homogeneity of background illumination in the Buridan arena using two different diffuser materials (paper and acryl-based covers of fluorescent ring lights) and compared these conditions to a newly designed Buridan LED arena displaying the same visual stimulus (stripes of the same color, width, and height) (Fig. 1d, Fig. 2c and supplemental Fig. S2c and S3c). We measured no significant differences between the group means of the two diffuser conditions and only minor group-based changes compared to the LED Buridan (supplemental Fig. S2c). We then tested the correlation of individual behavior across these conditions, as a measurement of behavioral consistency, expecting high correlations. Indeed, the different diffusers within the same arenas only had minor effects on the behavior of individual flies (Fig. 1d). Conversely, the individual response changed dramatically when the same fly was tested again in the LED arena, albeit presenting the same stimulus (Fig. 1d). A fly's attention and anxiety parameters quantified within the original arena did not allow for any prediction for the LED arena (Fig. 2c). Significant correlations between the LED arena and the original arenas were only measured for exploration parameters (Fig. 2c). This unpredictability of individual fly behavior across situations was once again particularly surprising since group-based performances remained similar (supplemental Fig. S2c). Finally, a detailed comparison of males and females revealed only quantitative but no qualitative differences across all parameters between the two sexes (supplemental Fig. S2 and supplemental Fig. S3).

Based on the surprising result that individuality (Gosling, 2008) of visual orientation behavior is more strongly influenced by the arena type (despite producing very similar group responses) and, only to a lesser degree, dependent on the visual cue (despite strong

504 differences in the group response), we set out to characterize the contribution of environmental
505 situations to individuality even more quantitatively. We therefore built a multiplatform high-
506 throughput assay (Indytrax) to quantitatively study the behavior of the same individual flies in
507 different environmental situations (Fig. 3, technical details supplemental Fig. S4).

508 Using Indytrax, we compared the behavioral parameters of each fly in eight different
509 environmental situations (Fig. 4, supplemental Fig. S6, S7, S8). The flies were tested in two
510 independent arenas (Buridan and Y-maze) at two different temperatures (23°C and 32°C,
511 supplemental Fig. S5) and under both light and dark conditions. Our analysis showed that
512 temperature significantly affected exploration parameters on the group mean level. As
513 expected, most animals tested were more explorative at higher than at lower temperatures
514 ((reviewed in: Gibert et al., 2016)) (supplemental Fig. S6). Despite these group changes,
515 individuals kept their rank within the group independent of the changed baseline activity. For
516 example, fly #1 was the least explorative, fly #2 exploration performance ranked medium, and
517 fly #3 the highest (Fig. 4a). The graphical analysis of exploration parameters (Fig. 4b)
518 confirmed that most individuals maintain their rank in the distribution under different
519 temperatures and light-dark conditions, whereas the individual distribution rank changed
520 between the different arena types. This relationship was less pronounced for attention
521 parameters. The detailed correlative analysis between individuals underscores these
522 observations (Fig. 4c and supplemental Fig. S7 and full analysis supplemental Fig. S8):
523 Amongst the exploration parameters, the percentage of time walked significantly correlated
524 between individuals (Pearson r=0.263-0.398) independently of temperature, illumination, and
525 arena. Walking speed was highly correlated between individuals (Pearson r=0.81, 0.825)
526 under temperature and illumination changes but uncorrelated in different arena types (Pearson
527 r=0.091). Vector strength was the most correlated attention parameter. The individual
528 correlations ranged from Pearson r=0.533 to -0197. Angular velocity significantly correlated for
529 temperature and illumination (Pearson r=0.246, 0.354) but not in different arenas (Pearson
530 r=0.087). The same is true for anxiety measured through centrophobicity (Pearson r=0.694,
531 0.740, 0.033). In summary, these data revealed that individuality measured in three traits is

532 mostly unaffected by temperature and illumination but strongly affected by the arena type. Our
533 analysis confirmed that even in situations with a large effect on the mean group behavior (like
534 temperature), individual behavioral consistency of idiosyncrasies remained high, while
535 conversely, other environmental situations like the arena type had little impact on the mean
536 but a massive effect on individual behavioral consistency (Fig. S6). Qualitatively similar results
537 leading to the same conclusions were obtained for both sexes (Fig. S6a, S7a) and two different
538 genotypes (Fig. S6b, S7b)

539 Next, we drastically modified the behavioral situation while keeping the visual stimulus
540 as constant as possible. We, therefore, decided to investigate the influence of a fly's modality
541 of locomotion (walking versus flying) on individuality. To do this, we designed a new virtual
542 flight arena for tethered flight utilizing the exact same LED panels as were used in the LED
543 Buridan arena (Fig. 5a-c and supplemental S9 for technical details), to maximize the similarity
544 of the visual context. This flight simulator tracked a fly's heading in real-time in response to
545 dynamic or static panoramic visual stimuli with high resolution (1.4° pixel size). This allowed
546 us to quantitatively compare the visual decisions of both walking and flying flies in response to
547 standard optomotor and Buridan-like stimuli (Fig. 5d-e). We first tested individuality in flying
548 flies over time under the same and a set of modified visual stimuli (Fig. 6, supplemental Fig.
549 S10 and S11). Each fly was tested over two consecutive days under three different visual
550 conditions (dark stripes on a bright background with either 50% or 100% contrast, and an
551 inverted Buridan with bright stripes on a dark background and 100% contrast) (Fig. 6a).
552 Overall, the flies showed some individuality in visual attention across days and contrast. This
553 was also true for the inverted Buridan stimulus, in which the flies oriented themselves toward
554 the dark areas, similar to previous results (Han et al., 2021). To allow a quantitative comparison
555 across behavioral traits between walking and flight behavior, we derived an adapted set of
556 parameters for exploration and attention quantification (exploration parameters: # of pauses,
557 Absolute angular velocity; attention parameters: Vector strength, Angular velocity, and Median
558 heading axial, Fig. 6b). The resulting analyses revealed individuality in flying flies (Fig. 6c).
559 Only the inversion of the Buridan stimulus resulted in variable angles towards the black

560 background on different days. However, it is remarkable that on a given day, each fly selected
561 an arbitrary heading that was kept for the entire experimental length (Fig. 6a). Again, the
562 quantitative analysis between males and females did not reveal qualitative differences (Fig.
563 S11).

564 After confirming that individuality also existed in flying flies, we tested how different
565 locomotion modalities affected a given animal's behavioral individuality. Behavioral parameters
566 of both walking and flying flies were quantified in response to the same panoramic LED screen
567 displaying an identical two-stripe Buridan stimulus (Fig. 7a, supplemental Fig. S12 and S13).
568 We expected one of three possible outcomes: 1. There is no consistency of individual
569 behavioral traits across flying and walking, 2. Only some behavioral traits are similar across
570 flying and walking. 3. The fly's individuality remains stable across the same visual cue,
571 independent of the locomotive modality. Subsequent quantitative analysis indeed revealed a
572 significant correlation for angular velocity between flying and walking flies (Fig. 7b), indicating
573 that a fly's attention towards a visual object is, to some degree, preserved independent of the
574 locomotor modality. In contrast, we found no statistically significant correlations for any of the
575 exploration parameters between flying and walking. Finally, a more detailed analysis revealed
576 mostly comparable results for male and female data (supplemental Fig. S12 and S13).

577 The data presented here reveal a hierarchical influence of different parameters within
578 the environmental context on individuality (Fig. 8): First, we conclude that time (at least within
579 the frame of days) has a negligible influence on individual behavioral responses (the basis of
580 the definition of animal individuality in a single situation), since we found consistency of
581 individual behavioral traits and parameters over time in both locomotor modalities, walking and
582 flying. Second, temperature had the second weakest impact on individuality (although only
583 tested for walking behavior). This contrasts the dramatically altered group mean responses, a
584 difference that can be explained by scaled individual responses in which individuals keep the
585 rank in the group. Third, the nature of the visual input appears to influence the individual
586 orientation responses but has little impact on the exploration parameters. Finally, we identified
587 the most critical situational environmental features that determine individual responses as both

588 the arena type and the locomotor modality (walking vs. flying). Therefore, we conclude that the
589 individuality of visually guided behaviors persists specifically in some traits across situations,
590 but the environmental context plays a prominent role in defining individual behavioral
591 responses.

592 To verify the results of our multiple correlative analyses, we took advantage of a
593 generalized linear model (GLM, Fig. 9). We first analyzed the effect of time, temperature,
594 vision, and arena on the mean group responses analogous to supplemental Fig. S2, S6, S10,
595 S12, (Fig. 9a). Our reanalysis of the walking data confirmed the temperature dependency of
596 activity parameters (Fig. S6). It also revealed effects on the group means by vision and arena
597 particularly for walking speed. The orientation parameter vector strength was similarly affected
598 by temperature vision and arena (see also supplemental Fig. S2, S6), while the position
599 parameter centrophobicity was strongest affected by the arena (see also supplemental Fig.
600 S2, S6). For flight parameters, the reanalysis of mean data revealed a strong effect of vision
601 on the orientation parameter vector strength and the heading parameter median heading axial
602 (see also supplemental Fig. S10). Our reanalysis, therefore, confirmed our previous analysis
603 of mean group data.

604 The next step of our reanalysis was to compare the rank changes of our flies across
605 situations analogous to the correlation analysis we had done (Fig. 2, 4, 6, 7). Our reanalysis
606 revealed significant changes in activity parameters and the orientation parameter vector
607 strength. In these parameters, the effect on the rank of each individual increases from time
608 over temperature, vision, and arena to the behavioral state. Confirming the data we found in
609 Fig. 2, 4, 6, 7, and 8. Also, the lack of a significant effect of the behavioral state for angular
610 velocity confirms our correlation analysis of Fig. 7 and 8.

611 Furthermore, we generated a GLM with ridge regression to show the effect of changing
612 environmental situations on individual rank differences (Fig, 9c). First, we converted the
613 individual mean values for every behavioral trait to within-group ranks (0 to 100). We then used
614 the GLM to predict the average change in rank for a fly when altering a single environmental
615 context. Each bar in Fig. 9c represents the predicted influence of changing a certain

environmental parameter on the persistence of each behavioral trait, where larger values indicate a larger influence on rank persistence and smaller values indicate less influence of the respective environmental context on rank persistence. Due to the response variable being in rank-points, the predicted rank shift due to changing the respective environmental context is the height of a bar in Fig. 9c added to the indicated intercept values. Based on our correlative analysis, we predicted a spectrum of context-dependencies of individual behavioral stability, where behavioral state > arena > vision > temperature > time in their ability to alter the persistence of individuality. The output of the GLM analysis supports that hypothesis, since calculated coefficients also indicate such a spectrum from rather stabilizing (e.g., time, temperature) to rather disruptive (arena, behavioral state). Our analysis shows that the effect was statistically significant for most environmental parameters.

For the activity parameters, time, temperature, and vision significantly stabilized individual phenotypical rank. In contrast, the arena and behavioral state significantly had a negative effect on rank stability. For the orientation parameter vector strength, we could fully replicate our previous findings that time had the strongest positive effect on consistency, followed by temperature. Vision had no significant impact. In contrast, the arena had a small negative effect consistency, while the behavioral state had a strong negative effect on behavioral consistency. In the second orientation parameter (angular velocity), a significant destabilizing effect was only found for the behavioral state. and for the positional parameter (centrophobicity), only vision had a significant effect on behavioral consistency.

Furthermore, as an additional step in our reanalysis, a hierarchical linear mixed-model analysis confirmed the findings of the previous analyses while providing a more complete and accessible overview of the influence of different environmental contexts on behavioral traits and the individual stability (repeatability) of these traits across environmental contexts. For walking as well as flight, the majority of behavioral traits showed significant repeatability across different contexts with ICCs on the order of about 0.1-0.6 for walking and 0.2-0.4 for flight (Fig. 10, see also supplementary table T3). When analyzing walking data, the highest ICCs were

644 measured for activity and orientation-related traits, indicating that flies tend to keep their
645 relative rank for these traits across environmental contexts. In contrast, centrophobicity as a
646 measure for anxiety showed much lower repeatability across different contexts (ICC near 0).
647 The pattern of repeatability was similar for flight traits, with high repeatability for activity traits
648 and low repeatability for the exploratory trait (heading). Both vector strength and the heading
649 showed only low ICCs across different contexts during flight, since the inversion of contrast
650 had a very strong effect on the flies' orientational choices (see Fig. 6), reducing rank stability
651 in these traits. Although the flight assays showed slightly lower ICCs overall, possibly reflecting
652 greater trial-to-trial noise, our key finding that individual behavioral traits are stable across
653 different environmental contexts was robust across behavioral modalities (walking vs flight).
654 Group-level behavior was shifted by environmental manipulations (e.g., increasing the
655 temperature led to an increase in mean activity in walking and flight assays). However,
656 individual differences were not erased by these shifts. E.g., in each context, flies that were
657 relatively less active than the average in one environmental context remained so in other
658 environmental contexts, therefore preserving rank order. Most environmental context effects
659 appeared as shifts in the intercept (group means) rather than changes in the rank order of
660 individual differences.

661 In summary, using three independent mathematical approaches, we have established a
662 hierarchy of different environmental situations on behavioral consistency. This data
663 demonstrates that temporal consistency is also prevalent in animals. Like humans also animals
664 have significant consistency across situations, but similar to humans different situations evoke
665 different behavioral responses, masking some measurable behavioral consistency.

Discussion

Our work presented here focused on the question of whether the combination of stable behavioral parameters ranging across different traits and therefore defining an animal's individuality are invariable across situations or whether they are re-shaped by different environmental contexts. This question is closely related to the questions in the human 'person-situation debate' (Mischel, 1968). Until now, in the neurosciences, individuality across situations has been largely ignored since many commonly used definitions of animal individuality only refer to the repeatability of behavior over time in a single environmental situation (Gosling, 2008). The contrary is true for mainly field and observation-based sciences such as ethology and behavioral ecology that have since decades acquired observations for (Boissy & Bouissou, 1995; Spoolder et al., 1996) or against (Coleman & Wilson, 1998; D'Eath & Burn, 2002) behavioral consistency across situations, with some of the most convincing work probably found in hermit crabs (Briffa et al., 2008; Mowles et al., 2012), blue tits (Herborn et al., 2010), and geese (Kralj-Fišer et al., 2007). Our work establishes animal individuality across situations under several tightly controlled laboratory conditions, revealing that animal individuality shares remarkable similarities to what has been described in human personality research. In agreement with Vansteelandt, 2004 our results are in line with the concept of the personality triad, emphasizing the interplay of individual, situation, and behavior (in humans: person, situation, and behavior) (Vansteelandt & Van Mechelen, 2004).

Our results confirm that under the same environmental situation and stimulus, animals produce inter-individually variable, but extremely consistent behavioral responses when being retested (Bell et al., 2009). Therefore, consistent and individually variable behaviors likely result from individual brain properties that persist over long timescales (in this paper days as shown in previous papers months (Linneweber et al., 2020)), contrasting random behavioral variations like sudden internal state variations. Hence, when presented with the same stimulus in the same situation, each individual responds variably but repetitively so, pointing towards a deterministic and hardwired basis of individual properties (Buchanan et al., 2015; Linneweber et al., 2020).

694 The variability of the situational environmental context makes individual animal
695 behavior in the wild much less predictable than that under laboratory conditions (Briffa &
696 Greenaway, 2011). In opposition to the vast human literature on the 'person-situation debate'
697 (Diener & Larsen, 1984; Fleeson, 2001; Mischel, 1968; Vansteelandt & Van Mechelen, 2004;
698 Weisbuch et al., 2010), the importance of environmental context in shaping individual animal
699 behavior remains descriptive (Kralj-Fišer et al., 2007) and experimentally largely unexplored,
700 with few exceptions (Briffa et al., 2008; Mowles et al., 2012; Versace et al., 2020; Werkhoven
701 et al., 2021). Here, we closed this gap in knowledge by quantitatively demonstrating how
702 situational environmental and locomotor context changes individual behavior and individuality
703 in animals. Our results demonstrate that situational environmental context has a pronounced
704 effect on individual behavioral responses, be it an alternative stimulus representation, a
705 different arena, or another locomotive modality.

706 Similar to the human literature (Mischel, 1968), the correlation coefficients are lower
707 across situations than in the same situation or environmental context. From this, we can
708 conclude that under more natural conditions with varying contexts, the consistency of individual
709 traits measured by behavioral parameters will be reduced but remain measurable; therefore,
710 for each situational context, the brain computes the appropriate behavior. This is like the
711 situation-behavior profile of the individual in the personality psychology literature (Mischel &
712 Shoda, 1995; Mischel & Shoda, 1998). Each time the individual is placed in the same
713 situational context, the same behavior will be evoked, in a different context, a modified
714 behavior. But despite these modifications, the individual brain properties computing the
715 response remain the same. In line with lower but measurable behavioral consistency across
716 situations , a vast literature demonstrates the importance of animal individual differences for
717 ecological communities under natural conditions (reviewed in: Sih et al., 2012; Takola &
718 Schielzeth, 2022).

719 Our quantitative analysis of the effect of environmental and locomotor context on
720 behavioral consistency revealed a hierarchy. As expected from animal and human studies, the
721 time frame of days had little effect on the behavioral outcome (Bell et al., 2009; Buchanan et

722 al., 2015; Linneweber et al., 2020; Mischel, 1968; Pantoja et al., 2016; Ross, 1977; Schuett et
723 al., 2011). The hierarchy revealed by our experiments argues for differences in the relevance
724 of environmental features for the traits we measured, which aligns with Mischel's strong or
725 weak situations (Mischel, 1973). Therefore, it is unsurprising that exploration can be best
726 measured across situations within experiments of walking flies, and attention towards a
727 stimulus can be measured across movement modalities. Our quantitative analysis
728 demonstrates that situational context can be the most significant factor in determining the
729 individual behavioral outcome, even in a per-design visual assay. This argues that individual
730 behavior is determined by the entirety of the situation consisting of both the stimulus and the
731 environmental context. For each situation, each individual manifests its individual behavior.

732 In the future, it will be important to investigate which individual neurophysiological
733 responses change when tested under exactly the same stimulus, but different situations. A
734 systematic analysis of relevant circuit elements for different behaviors will allow for determining
735 the exact neuronal substrates underlying individual behavioral computations within a fly's or
736 other animals' brains. This future research on animal models will provide important new insight
737 into the 'person-situation debate'.

738 On a more practical level, the importance of the situational environmental context for
739 shaping individual behavioral outcomes is also very important when comparing the results of
740 different research groups when using similar behavioral paradigms. In many instances, it is
741 impossible to replicate all components of a specific assay, let alone the conditions of the
742 experimental room. Our results show that such details substantially impact individual
743 behavioral responses and contribute to errors in replicating the results from another lab
744 (Crabbe et al., 1999; Lithgow et al., 2017). Only meticulous and detailed reporting of as many
745 environmental features as possible will hopefully alleviate some of these problems in the future.
746 Also, in terms of statistics, using well-established approaches can be an advantage. The
747 hierarchical mixed-model analysis provides a more complete and accessible overview of the
748 findings in our study, making it more comparable to previous findings in behavioral ecology
749 (Dingemanse & Dochtermann, 2013).

In conclusion, our work confirms that animals, including flies, have, like humans, individuality across situations. Similar to humans, animal individuality across situations is also marked by lower correlation coefficients than repetitions of a single situation. The individual is stable across situations producing individualistic behavior through an interaction with the situation. This involves a hierarchy of influence of different environmental features on the predictability of behavior across situations.

Acknowledgements

The authors thank the Bloomington stock center and Eugenia Chiappe for fly stocks and reagents. This work was supported by the Deutsche Forschungsgemeinschaft (DFG) through the DFG research unit 5289 RobustCircuit (G.A.L, M.F.W), through grants LI 2640/1-1, FOR5289 LI 2640/2-1 (G.A.L.), WE 5761/4-1 (M.F.W.), SPP 2205 (M.F.W.), through AFOSR grants FA9550-19-1-7005 / FA 8655-23-1-7049 (M.F.W.), and with support from the Fachbereich Biologie, Chemie & Pharmazie of the Freie Universität Berlin, as well as the Division of Neurobiology at Freie Universität Berlin. We acknowledge support by the Open Access Publication Fund of Freie Universität Berlin. We thank members of the Linneweber and Wernet labs, Randolf Menzel and Robin Hiesinger for helpful discussions.

Author Contributions

Conceptualization, T.F.M., G.A.L. and M.F.W.; Methodology, T.F.M., G.A.L. and M.F.W.; Investigation, T.F.M., C.K., M.A.H., F.F., T.M.; Resources, M.F.W.; T.F.M., G.A.L. and M.F.W.; Supervision, G.A.L. and M.F.W.; Funding Acquisition, M.F.W. and G.A.L

Declaration of Interests

The authors declare no competing interests.

Figure 1:

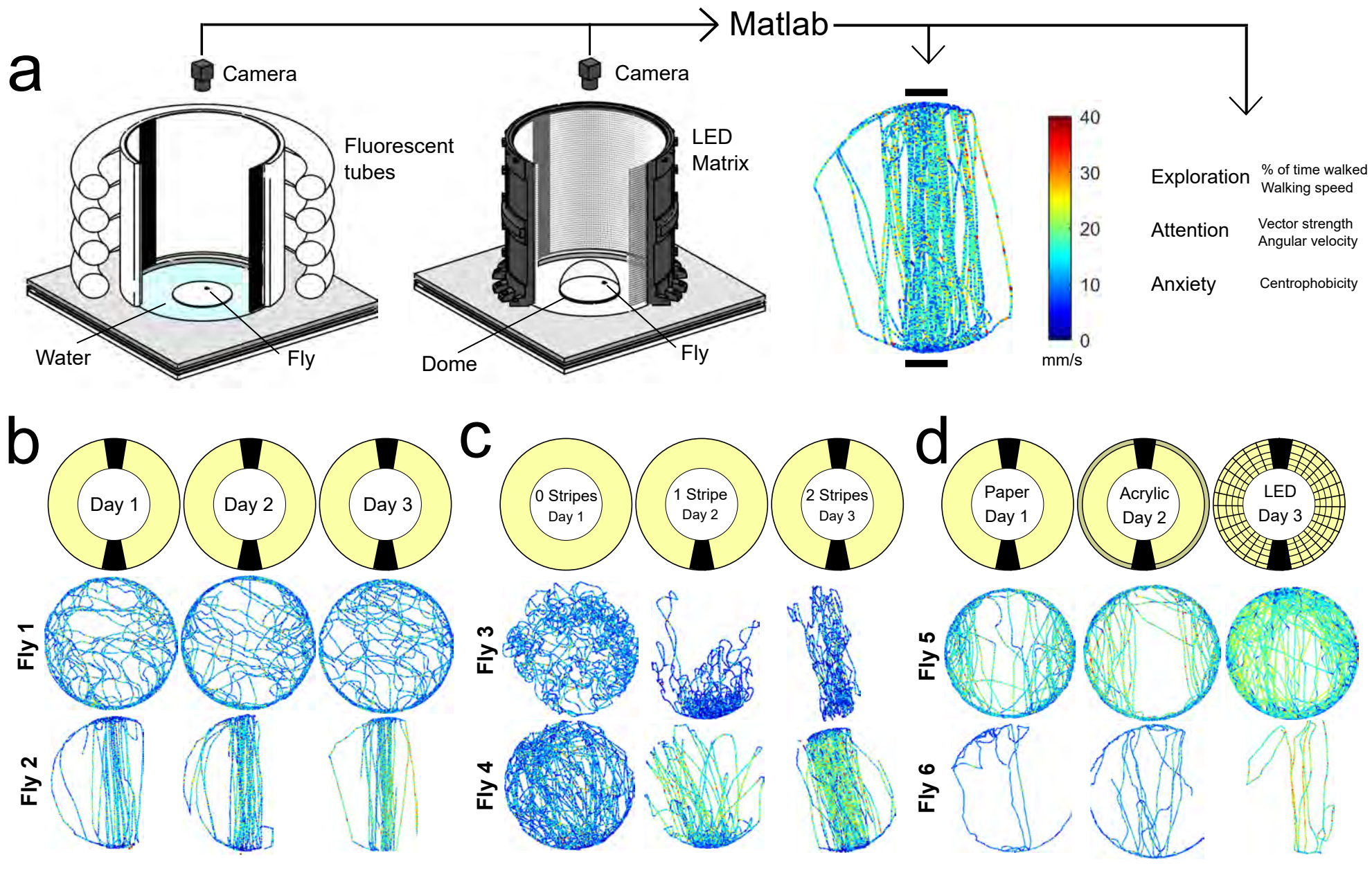
a
Matlab
Camera
Camera
Fluorescent tubes
LED Matrix
Water
Fly
Dome
Fly
40
30
20
10
0
mm/s
Exploration
% of time walked
Walking speed
Attention
Vector strength
Angular velocity
Anxiety
Centrophobicity
b
Day 1
Day 2
Day 3
Fly 1
Fly 2
c
0 Stripes Day 1
1 Stripe Day 2
2 Stripes Day 3
Fly 3
Fly 4
d
Paper Day 1
Acrylic Day 2
LED Day 3
Fly 5
Fly 6

Figure legends

Fig. 1: Setups for studying individuality walking flies. **a** Overview of a classical (left, fluorescent tubes) and LED (middle) Buridan assay (behavioral platform diameter = 120mm). A MATLAB script provides single fly tracking and analysis of behavioral key components (right). **b-d** persistence of individual walking patterns across time (**b**), different stripe numbers (**c**), and changes in background illumination (**d**).

Figure 2:

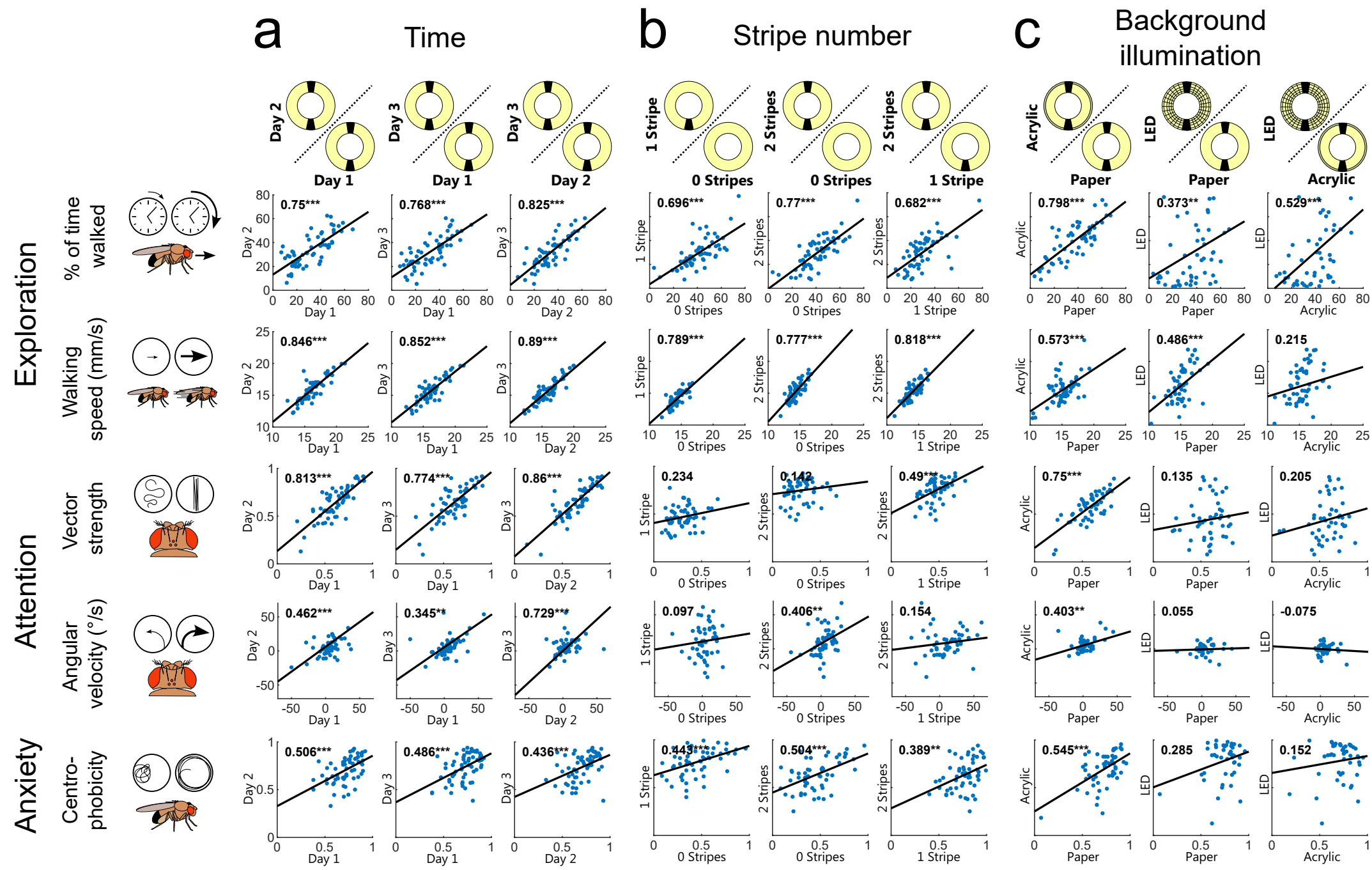
a
Time
b
Stripe number
c
Background illumination
Day 2
Day 3
Day 3
1 Stripe
2 Stripes
2 Stripes
Acrylic
LED
LED
Day 1
Day 1
Day 2
0 Stripes
0 Stripes
1 Stripe
Paper
Paper
Acrylic
Exploration
% of time walked
0.75***
0.768***
0.825***
0.696***
0.77***
0.682***
0.798***
0.373**
0.529***
Walking speed (mm/s)
0.846***
0.852***
0.89***
0.789***
0.777***
0.818***
0.573***
0.486***
0.215
Attention
Vector strength
0.813***
0.774***
0.86***
0.234
0.142
0.49***
0.75***
0.135
0.205
Angular velocity (°/s)
0.462***
0.345**
0.729***
0.097
0.406**
0.154
0.403**
0.055
-0.075
Anxiety
Centro-phobicity
0.506***
0.486***
0.436***
0.443***
0.504***
0.389**
0.545***
0.285
0.152

Fig. 2: Individual traits of walking flies persist over time but depend on the visual scenery. **a-c** Correlation of key behavioral parameters over time (n=60) (**a**), different stripe numbers (n=57) (**b**), and changes in background illumination (n=54) (**c**). Correlation coefficients are displayed in the upper left corner of each plot. *=p<0.05, **=p<0.01, ***=p<0.001, for detailed fly numbers per experimental condition, see supplemental Fig. S2.

Figure 3:

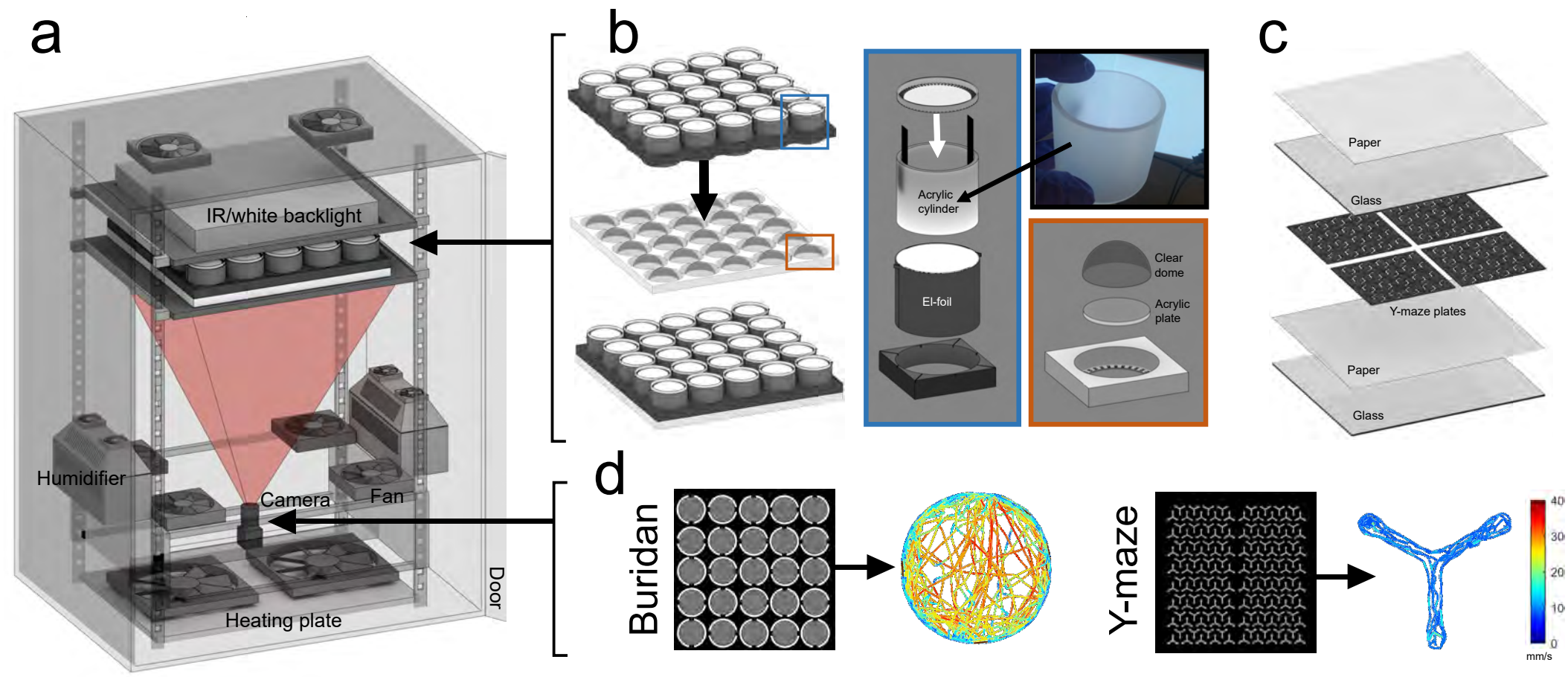
a
IR/white backlight
Humidifier
Camera
Fan
Heating plate
Door
b
Acrylic cylinder
El-foil
Clear dome
Acrylic plate
c
Paper
Glass
Y-maze plates
Paper
Glass
d
Buridan
Y-maze
40
30
20
10
0
mm/s

Fig. 3: A high-throughput assay for studying the influence of temperature, illumination, and arena shape on individuality. **a** Setup overview. Flies are filmed from below against a near-infrared backlight and are walking within a 5x5 array of small Buridan chambers (**b**) or one of up to 144 Y-maze arenas (**c**). The setup is housed within a temperature- and humidity-controlled enclosure (600 x 450 x 820 mm). The provided MATLAB code corrects lens distortions, automatically detects the arenas, and tracks each fly's position over time, allowing for generating high-throughput single-fly behavioral data (**d**). See Materials and Methods:Setup 2: IndyTrax multi-arena platform for details.

Figure 4:

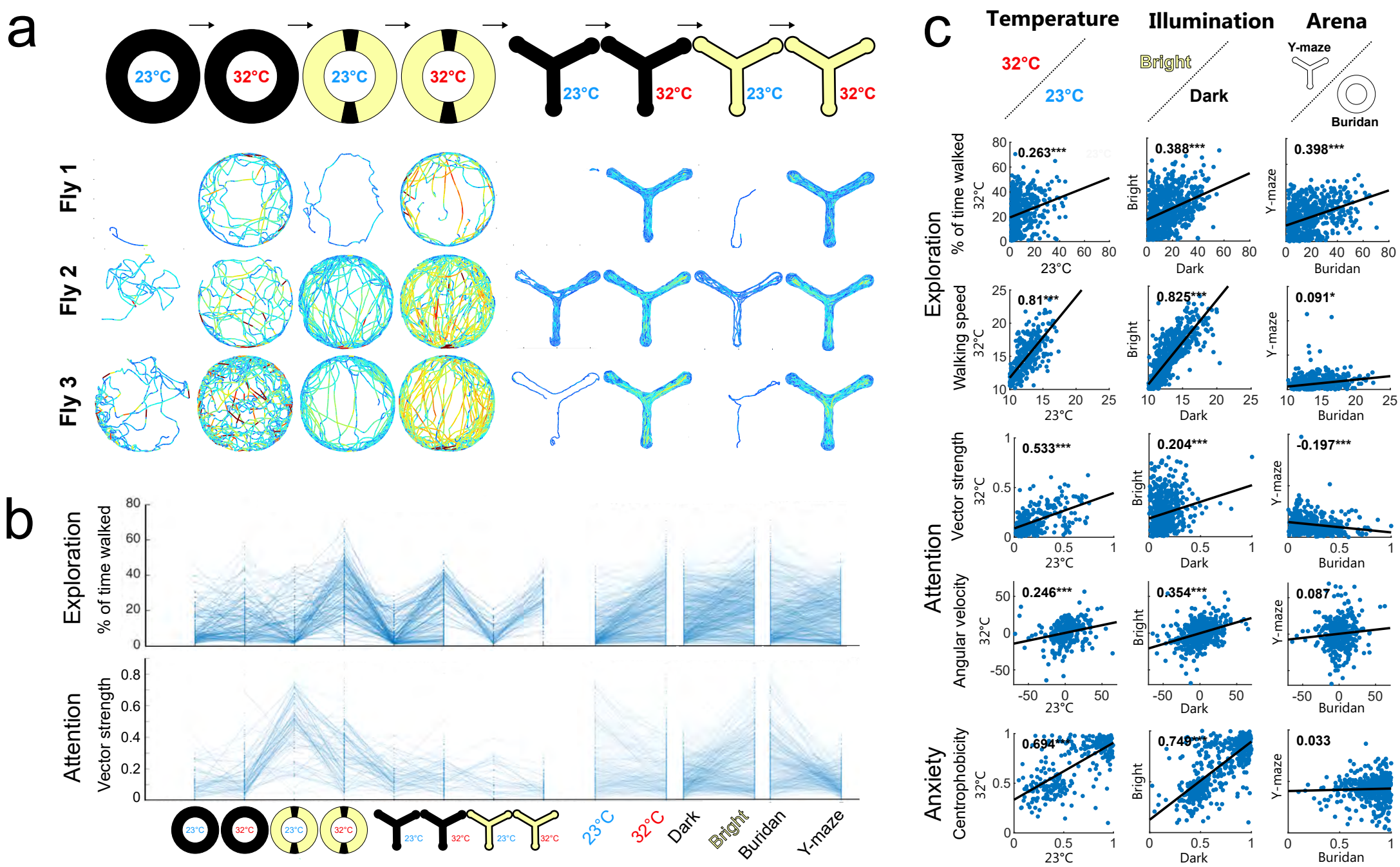
a
23°C
32°C
Fly 1
Fly 2
Fly 3
b
Exploration
% of time walked
Attention
Vector strength
Dark
Bright
Buridan
Y-maze
c
Temperature
Illumination
Arena
Y-maze
Buridan
Exploration
% of time walked
Walking speed
Attention
Vector strength
Angular velocity
Anxiety
Centrophobicity
0.263***
0.388***
0.398***
0.81***
0.825***
0.091*
0.533***
0.204***
-0.197***
0.246***
0.354***
0.087
0.694***
0.748***
0.033

Fig. 4: The influence of temperature, illumination, and arena shape on individuality in walking flies. **a** Individuality in walking patterns across different temperatures, illumination, and arena type. Diameter circular arena = 49mm, arm length from center Y-maze = 13.5mm. **b** changes in the % of time walked and vector strength for all tested flies depending on environmental conditions (n=400). Right: data grouped by temperature, illumination, and arena. **c** Correlation of key behavioral parameters across temperature, illumination, and arena type (n=400). For detailed fly numbers per experimental condition, see supplemental Fig. S6.

Figure 5:

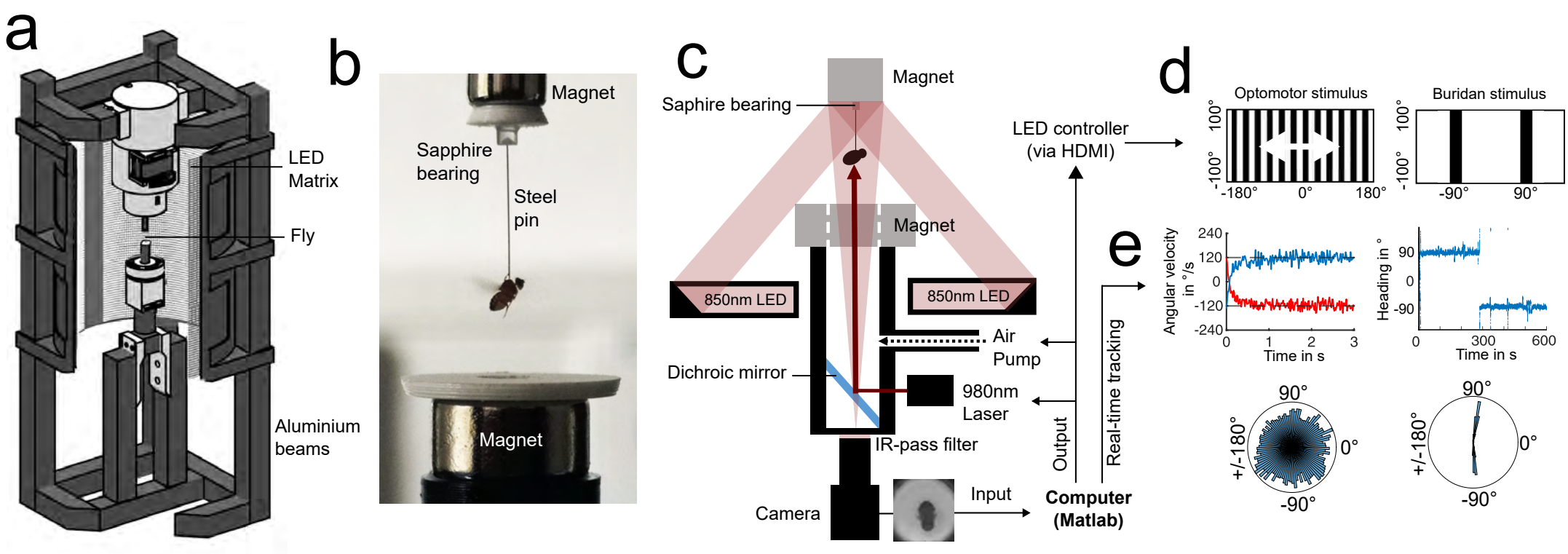
a
LED
Matrix
Fly
Aluminium
beams
b
Magnet
Sapphire
bearing
Steel
pin
Magnet
c
Magnet
Saphire bearing
Magnet
850nm LED
850nm LED
Air
Pump
Dichroic mirror
980nm
Laser
IR-pass filter
Camera
Input
Output
Real-time tracking
LED controller
(via HDMI)
Computer
(Matlab)
d
Optomotor stimulus
Buridan stimulus
100°
-100°
-180°
0°
180°
-90°
90°
e
Angular velocity
in °/s
240
120
0
-120
-240
0
1
2
3
Time in s
Heading in °
90
0
-90
0
300
600
Time in s
90°
+/-180°
0°
-90°
90°
+/-180°
0°
-90°

Fig. 5: A virtual flight simulator for studying individuality in flying flies. **a** Setup overview (225 x 225 x 600 mm). Flies are glued to a steel pin and placed in a magneto-tether surrounded by an LED matrix for stimulus presentation. **b** Close-up photo of a tethered flying fly. **c** Schematic setup overview. Flies are filmed from below through an IR-pass filter against near-infrared back illumination. A connected pump provides air puffs to reinitiate flight if necessary. We provide a mounting port for an optional IR-laser for heat punishment via a dichroic mirror. **d** A MATLAB script controls stimulus presentation (optomotor or Buridan stimulus) with an angular extent of 360° azimuthally and 100° vertically and provides simultaneous real-time tracking of flight-heading over 360° (**e**). Before an experiment, each fly's ability to rotate was tested using a 120°/s CW or CCW stripe rotation (optomotor stimulus), resulting in measured rotational flight movements close to the rotational velocity of the stripe pattern (**e**, upper left) and uniform distribution of angles (**e**, lower left). This was followed by each fly flying under the Buridan stimulus for 10min (**d**, right) and an analysis of heading choices (**e**, upper right) and their angular distribution (**e**, lower right).

Figure 6:

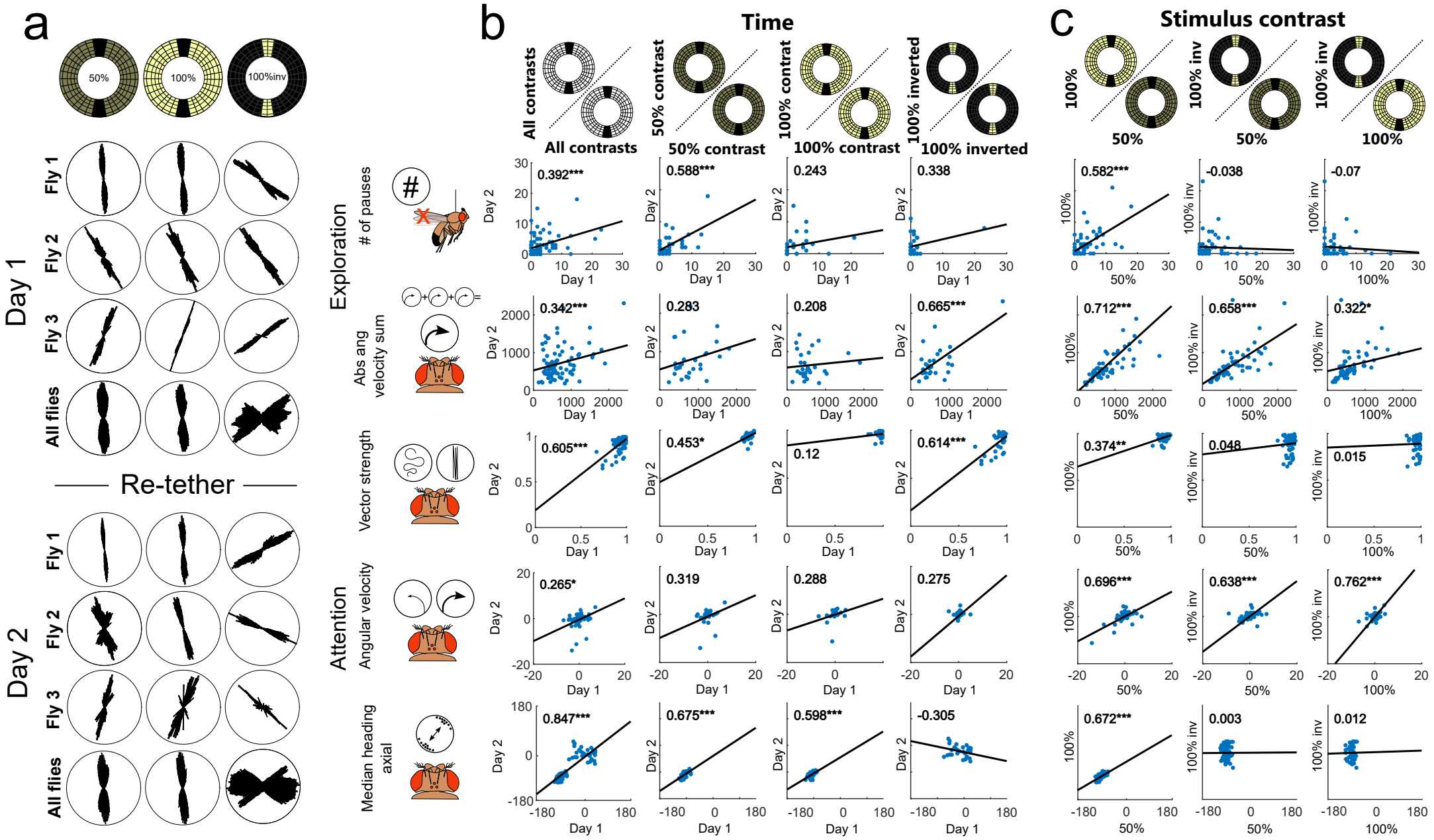
a
50%
100%
100%inv
Day 1
Fly 1
Fly 2
Fly 3
All flies
Re-tether
Day 2
Fly 1
Fly 2
Fly 3
All flies
b
Time
All contrasts
50% contrast
100% contrast
100% inverted
Exploration
# of pauses
Abs ang velocity sum
Vector strength
Attention
Angular velocity
Median heading axial
Day 1
Day 2
0.392***
0.588***
0.243
0.338
0.342***
0.283
0.208
0.665***
0.605***
0.453*
0.12
0.614***
0.265*
0.319
0.288
0.275
0.847***
0.675***
0.598***
-0.305
c
Stimulus contrast
100%
50%
100% inv
0.582***
-0.038
-0.07
0.712***
0.658***
0.322*
0.374**
0.048
0.015
0.696***
0.638***
0.762***
0.672***
0.003
0.012

Fig. 6: Individual traits of flying flies persist over time but depend on the visual scenery. **a** Angular histograms show the persistence of individual heading choices over consecutive days and across different contrast ratios. **b,c** Correlation of key behavioral parameters over time (n=30) (**b**) and depending on changes in visual contrast (n=30) (**c**).

Figure 7:

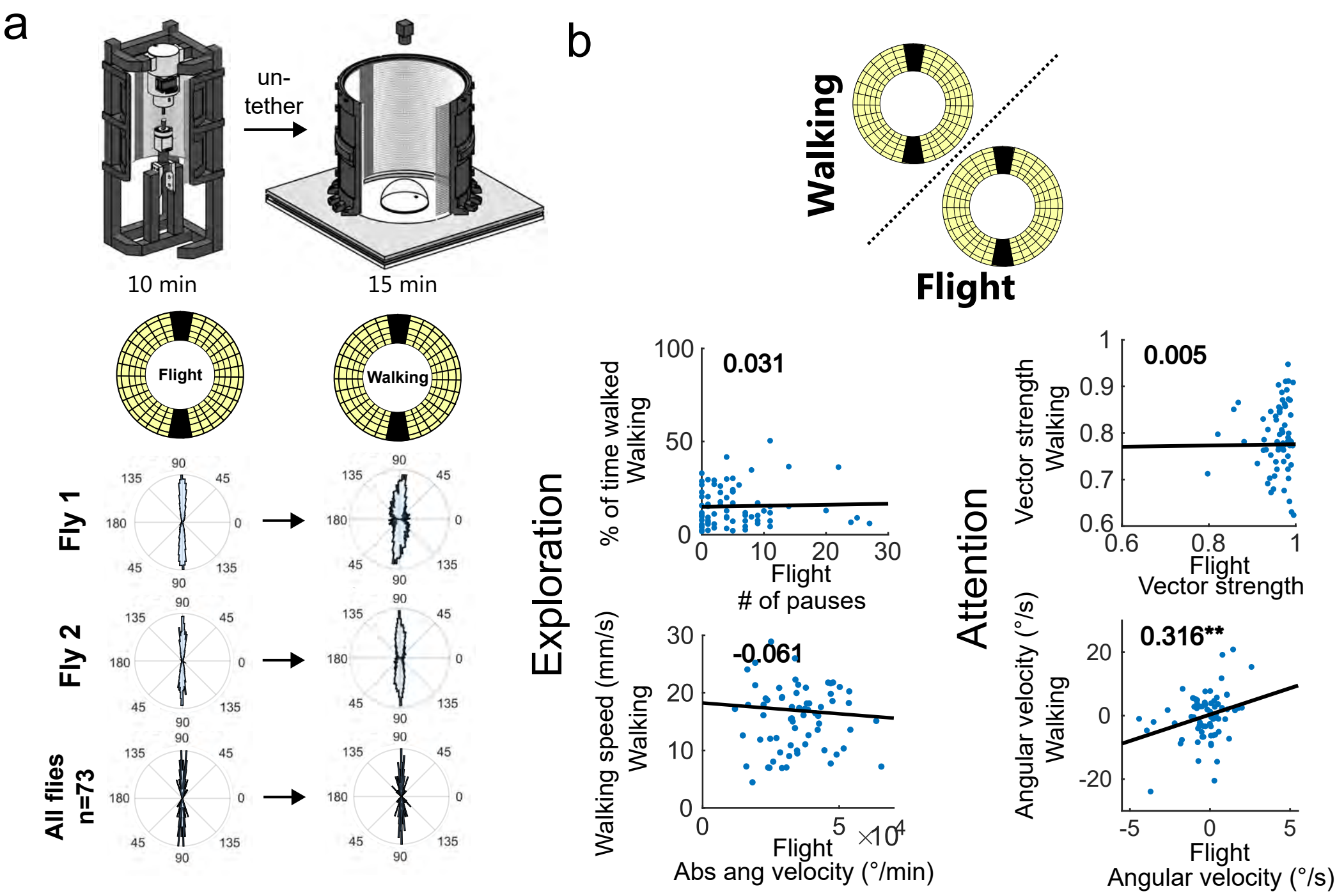
a
un-
tether
10 min
15 min
Flight
Walking
Fly 1
Fly 2
All flies
n=73
b
Walking
Flight
Exploration
Attention
0.031
% of time walked
Walking
Flight
# of pauses
0.005
Vector strength
Walking
Flight
Vector strength
-0.061
Walking speed (mm/s)
Walking
Flight
Abs ang velocity (°/min)
0.316**
Angular velocity (°/s)
Walking
Flight
Angular velocity (°/s)

Fig. 7: Visual attention persists across different behavioral states. **a** Experimental overview. Flies were untethered after flying within the flight simulator for 10 min (left) and walking for 15 min (right) under the same Buridan stimulus (stripe size=11°). Single fly data (middle) and group data (bottom) reveal stripe fixation behavior when walking and during flight. **b** Correlation of key behavioral parameters depending on the behavioral state (flight=x-axis, walking=y-axis, n=73).

Figure 8:

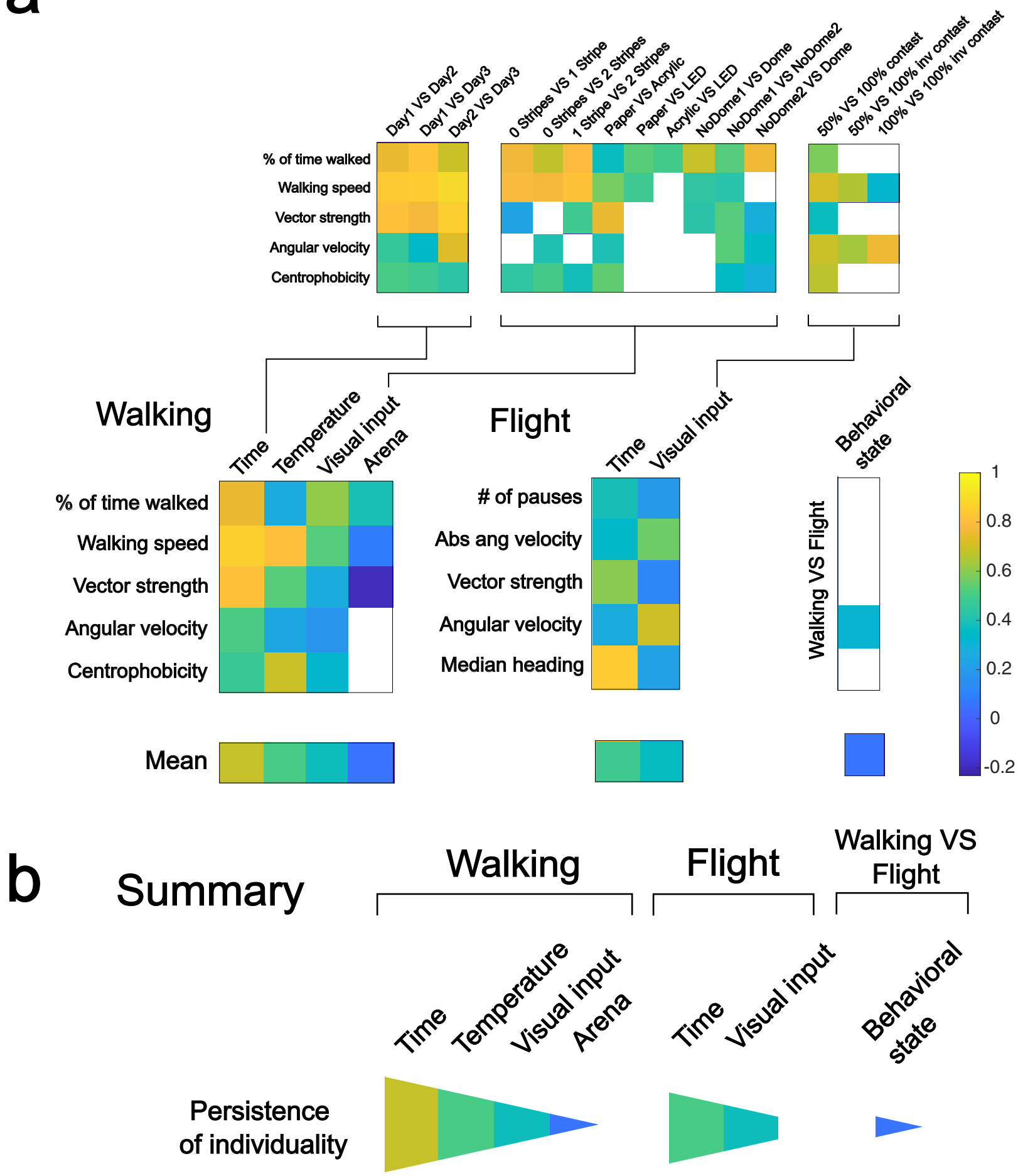
a
Day1 VS Day2
Day1 VS Day3
Day2 VS Day3
0 Stripes VS 1 Stripe
0 Stripes VS 2 Stripes
1 Stripe VS 2 Stripes
Paper VS Acrylic
Paper VS LED
Acrylic VS LED
NoDome1 VS Dome
NoDome1 VS NoDome2
NoDome2 VS Dome
50% VS 100% contast
50% VS 100% inv contast
100% VS 100% inv contast
% of time walked
Walking speed
Vector strength
Angular velocity
Centrophobicity
Walking
Time
Temperature
Visual input
Arena
Flight
Time
Visual input
Behavioral state
# of pauses
Abs ang velocity
Vector strength
Angular velocity
Median heading
Walking VS Flight
Mean
1
0.8
0.6
0.4
0.2
0
-0.2
b
Summary
Walking
Flight
Walking VS Flight
Time
Temperature
Visual input
Arena
Time
Visual input
Behavioral state
Persistence of individuality

Fig. 8: A hierarchy of environmental and behavioral contexts based on their influence on individuality. **a** Overview summarizing correlation coefficients ($p<0.05$) for key behavioral parameters depending on behavioral context, time, temperature, and visual input. **b** Quantification of the influence of behavioral and environmental contexts on the persistence of individuality.

Absolute individual difference walking

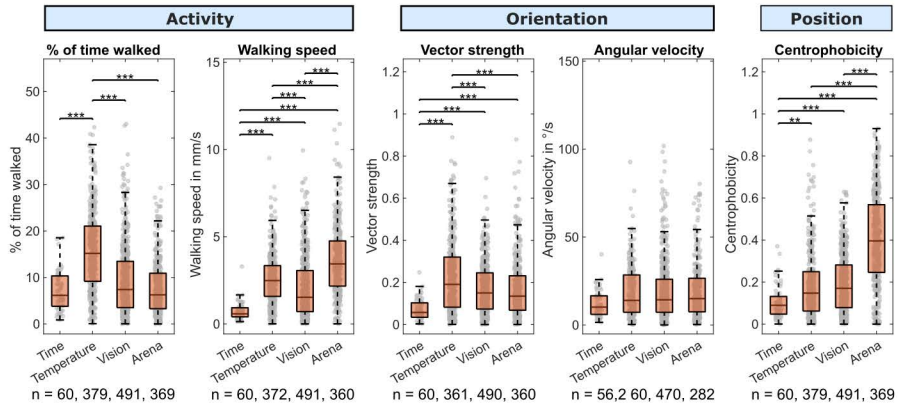

Absolute individual difference flight

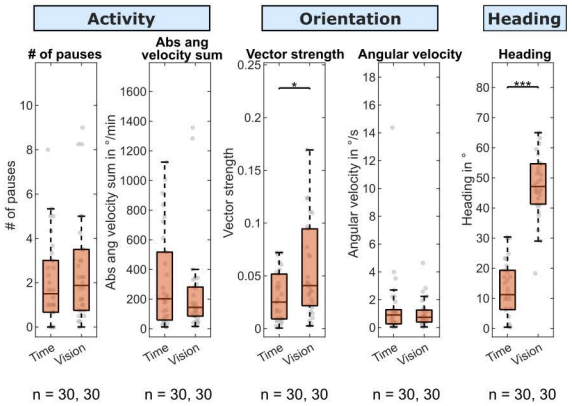

Absolute individual rank difference walking + flight

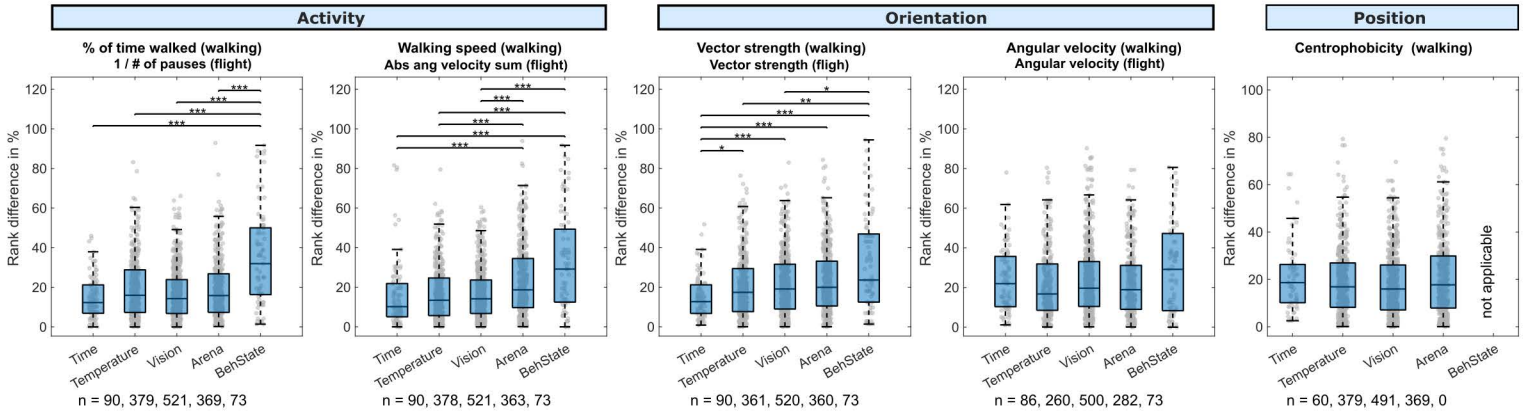

Regression model individual rank difference walking + flight

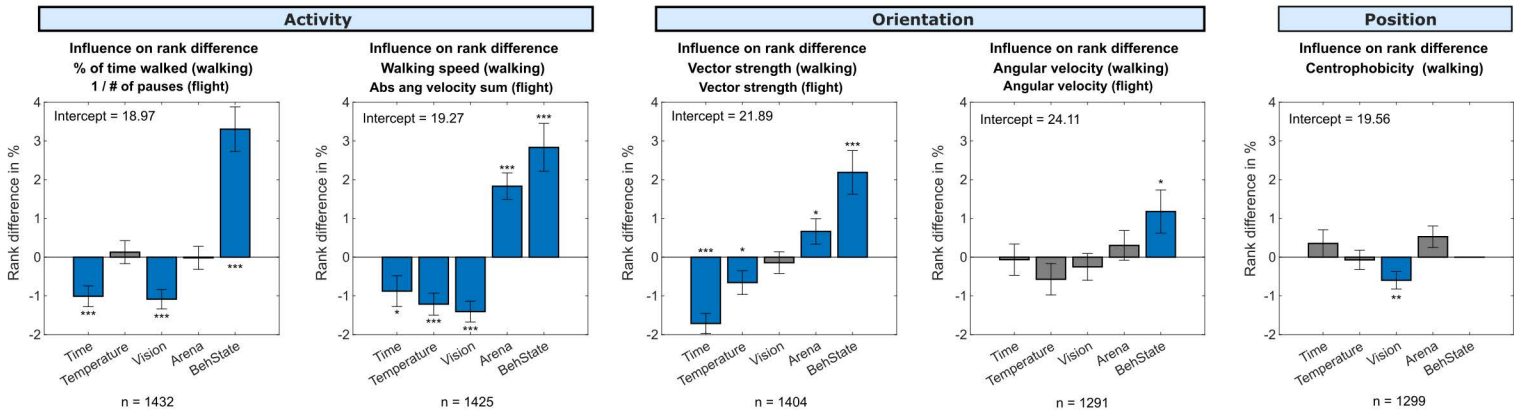

Fig. 9: A generalized linear model to demonstrate individuality across situations. **a** The difference of individual behavioral parameters for walking (left) and flight (right) when changing environmental conditions (time, temperature, vision, arena). Significance: *p<0.05, **p<0.01, ***p<0.001. **b** The difference of rank (in %) within the tested groups (walking and flight combined) when changing environmental conditions. Smaller rank differences indicate a lower influence of the environmental parameter on the persistence of individuality. Significance: *p<0.05, **p<0.01, ***p<0.001. **c** Generalized linear model (ridge regression) showing the influence of changing environmental parameters on individual rank differences within the tested group (individuality) using the data in **b**. Significance: *p<0.05, **p<0.01, ***p<0.001. Non-significant environmental parameters are shaded in grey.

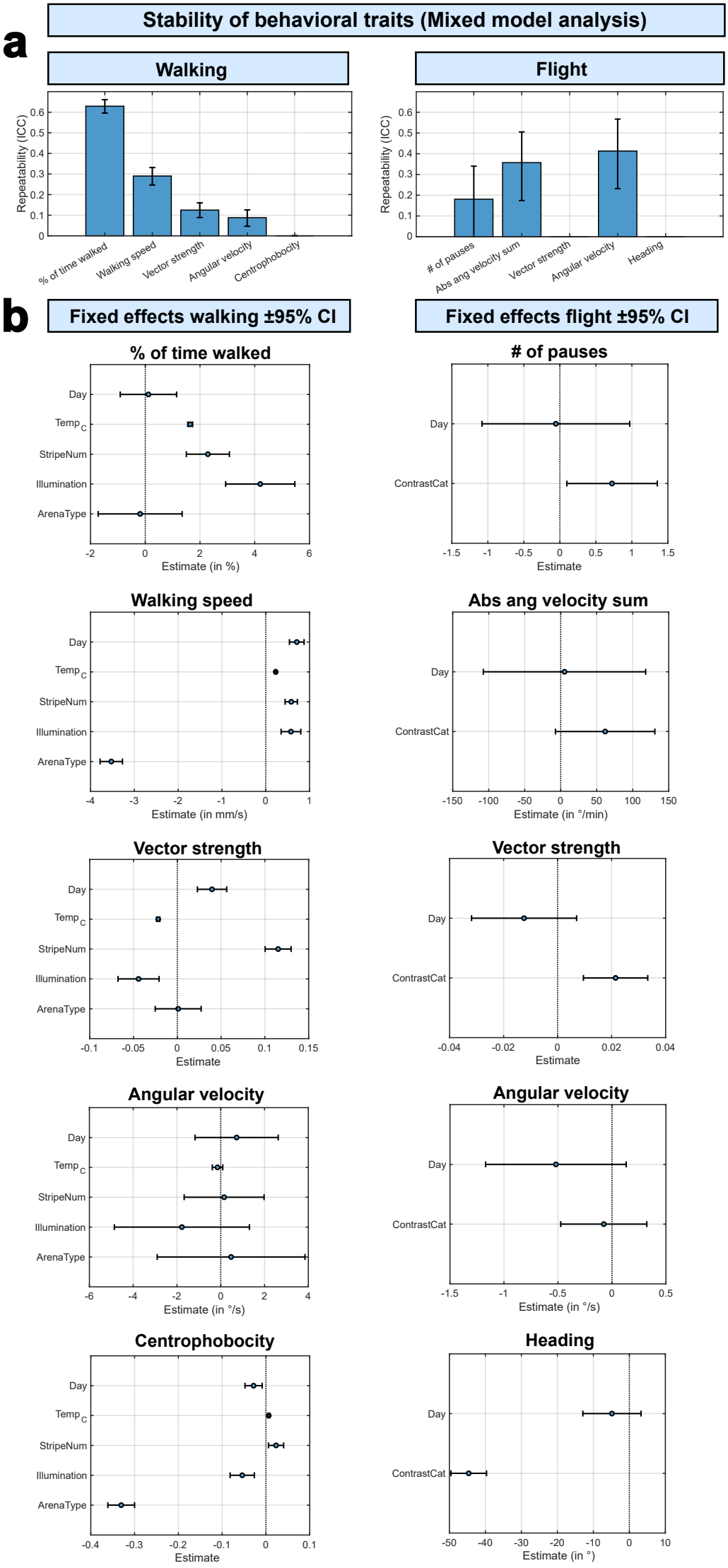
a
Stability of behavioral traits (Mixed model analysis)
Walking
Flight
Repeatability (ICC)
% of time walked
Walking speed
Vector strength
Angular velocity
Centrophobocity
# of pauses
Abs ang velocity sum
Heading
b
Fixed effects walking ±95% CI
Fixed effects flight ±95% CI
Day
Temp C
StripeNum
Illumination
ArenaType
ContrastCat
Estimate (in %)
Estimate (in mm/s)
Estimate (in °/min)
Estimate
Estimate (in °/s)
Estimate (in °)

Fig. 10: Hierarchical linear mixed-model analysis. **a** Repeatability across behavioral context of five walking (left) and five flight (right) behavioral traits, as measured via intraclass correlation coefficient (ICC). Bars indicate ICC estimates and whiskers show 95% confidence intervals (CI, obtained via 1000x bootstrapping, for details, see methods section). High ICC values indicate stronger persistence of individual traits across environmental contexts. Number of observations from left to right: 2983, 2912, 2666, 2099, 2987 (walking), 180, 180, 180, 180, 180 (flight). **b** Fixed-effect estimates and 95% confidence intervals (whiskers) from hierarchical mixed-models for each behavioral trait (left: walking, right: flight). For each modified environmental context (predictors, y-axes) the estimated effects are indicated with points (in units associated with the respective trait) with whiskers representing 95% confidence intervals. Positive estimates indicate that the behavioral trait increases by the indicated values with the predictor increasing one step and vice versa. Predictors were categorized numerically: 1-3 days, 25°-32°C, 0-2 stripes, light off (0) light on (1), round arena (0) y-maze (1). For a detailed overview of fixed-effects, see supplementary table T3.

Supplemental figure S1:

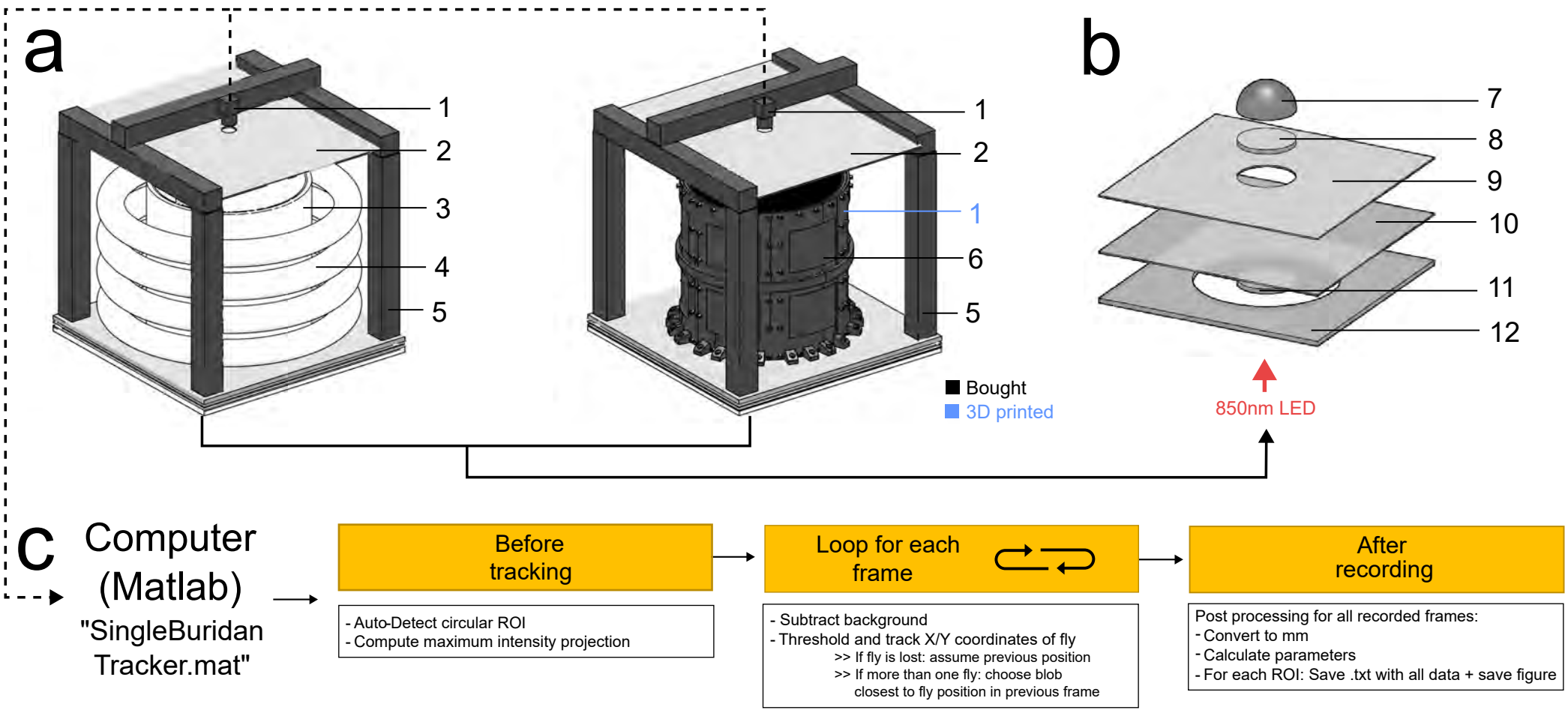

Supplemental figure legends

Supplemental Fig. S1: Construction of Buridan assays. **a** Two different types of Buridan assays (fluorescent tubes left, flexible LED matrix right) and the parts necessary for construction. Part numbers are referenced in supplemental table T2 and for 3D printed parts under github.com/LinneweberLab/Mathejczyk_2024_eLife_Individuality for replication. Black numbers indicate off-the-shelve parts; blue numbers indicate 3D-printed parts. **b** construction of Buridan bottom plates. An 850nm LED strip is wrapped around a translucent acrylic disk (11), providing homogeneous near-infrared background illumination from below. **c** schematic illustration of the tracking procedure. The provided MATLAB script automatically reads video frames, tracks the X- and Y-coordinates of individual flies over time, and saves data for further analysis.

Supplemental figure S2:

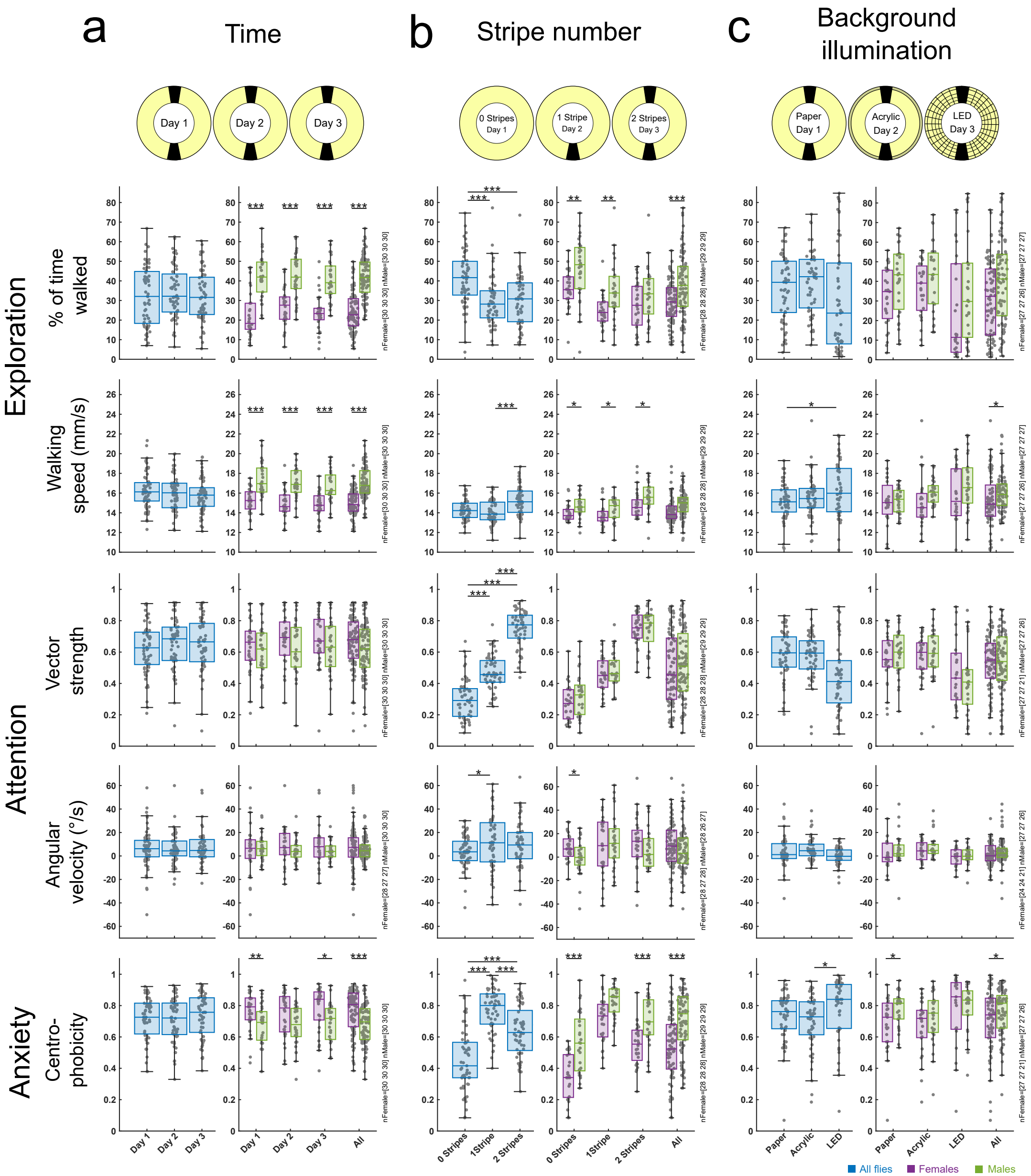

Supplemental Fig. S2: Group responses over time, varying stripe numbers and background illumination. **a-c** Boxplots illustrating key behavioral parameters for the whole group (blue) and separately for females/males (green/magenta) over time (**a**), varying stripe numbers (**b**) and background illumination (**c**). Animal numbers are indicated next to each plot.

Supplemental figure S3:

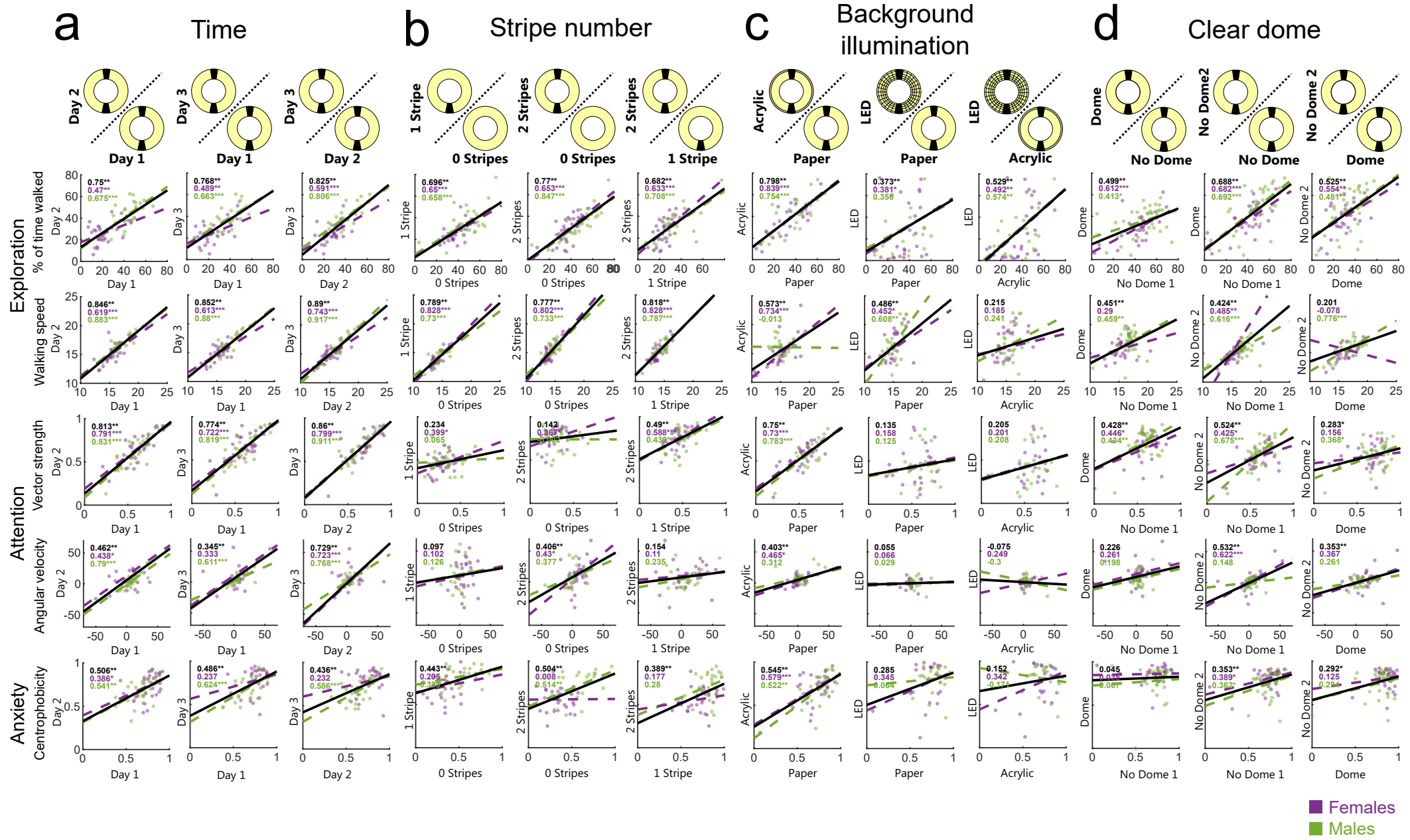

Supplemental Fig. S3: Sex-specific differences in individual traits. **a-d** Correlation of key behavioral parameters for females and males over time (**a**), different stripe numbers (**b**), changes in background illumination (**c**), and depending on the usage of a clear dome around the arena (**d**). Magenta=females, green=males. Correlation coefficients are displayed in the upper left corner of each plot. *=$p<0.05$, **=$p<0.01$, ***=$p<0.001$, for detailed fly numbers per experimental condition, see supplemental Fig. S2.

Supplemental figure S4:

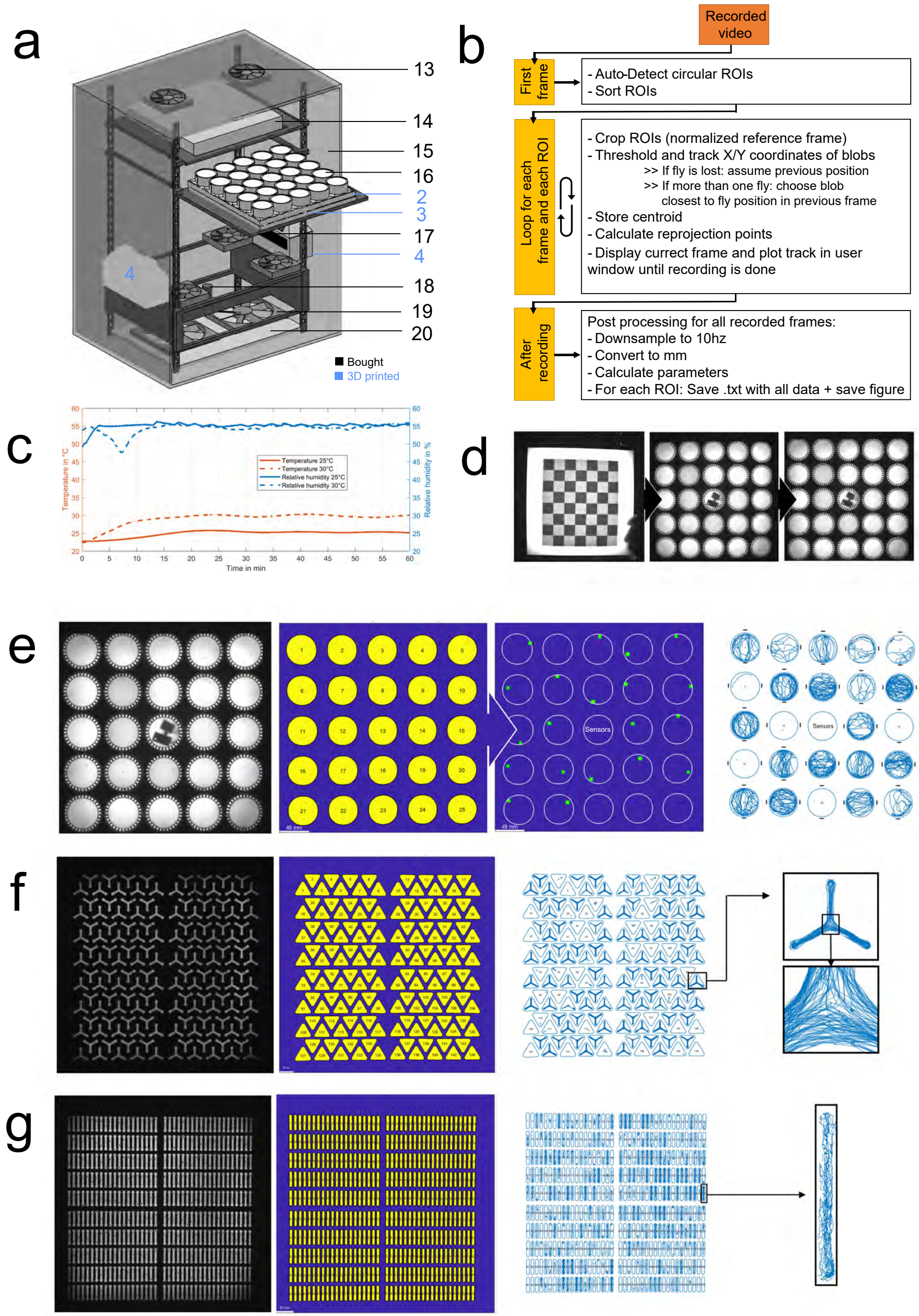

Supplemental Fig. S4: Construction of a high-throughput assay for studying the influence of temperature, illumination, and arena shape on individuality. **a** Overview of parts necessary for constructing the assay. Part numbers are referenced in supplemental table T2 and for 3D printed parts under github.com/LinneweberLab/Mathejczyk_2024_eLife_Individuality for replication. Black numbers indicate off-the-shelve parts; blue numbers indicate 3D-printed parts. **b** Schematic illustration of the tracking procedure. The provided MATLAB script automatically reads video frames, detects single arenas, tracks the X- and Y-coordinates of individual flies over time, and saves data for further analysis. **c** Exemplary temperature- and humidity curves were measured within the center arena during heat-up to 25 and 30°C, respectively. Stable plateaus are reached after ~20min. **d** The camera was calibrated using the MATLAB calibration toolbox. The provided MATLAB script uses these camera parameters to correct lens distortion artifacts during tracking. **e** Screenshots of the tracking procedure using the multi-Buridan assay. Arenas are detected automatically, and individual flies get thresholded after background subtraction, resulting in reliable trajectories of each individual fly. **f** Same as **e**, but for the Y-maze assay. The box on the right shows an enlarged depiction of a single arena. **g** Same as **e**, but for linear assays, demonstrating the usability of the setup with other arena shapes. The box on the right shows an enlarged depiction of a single arena.

Supplemental figure S5:

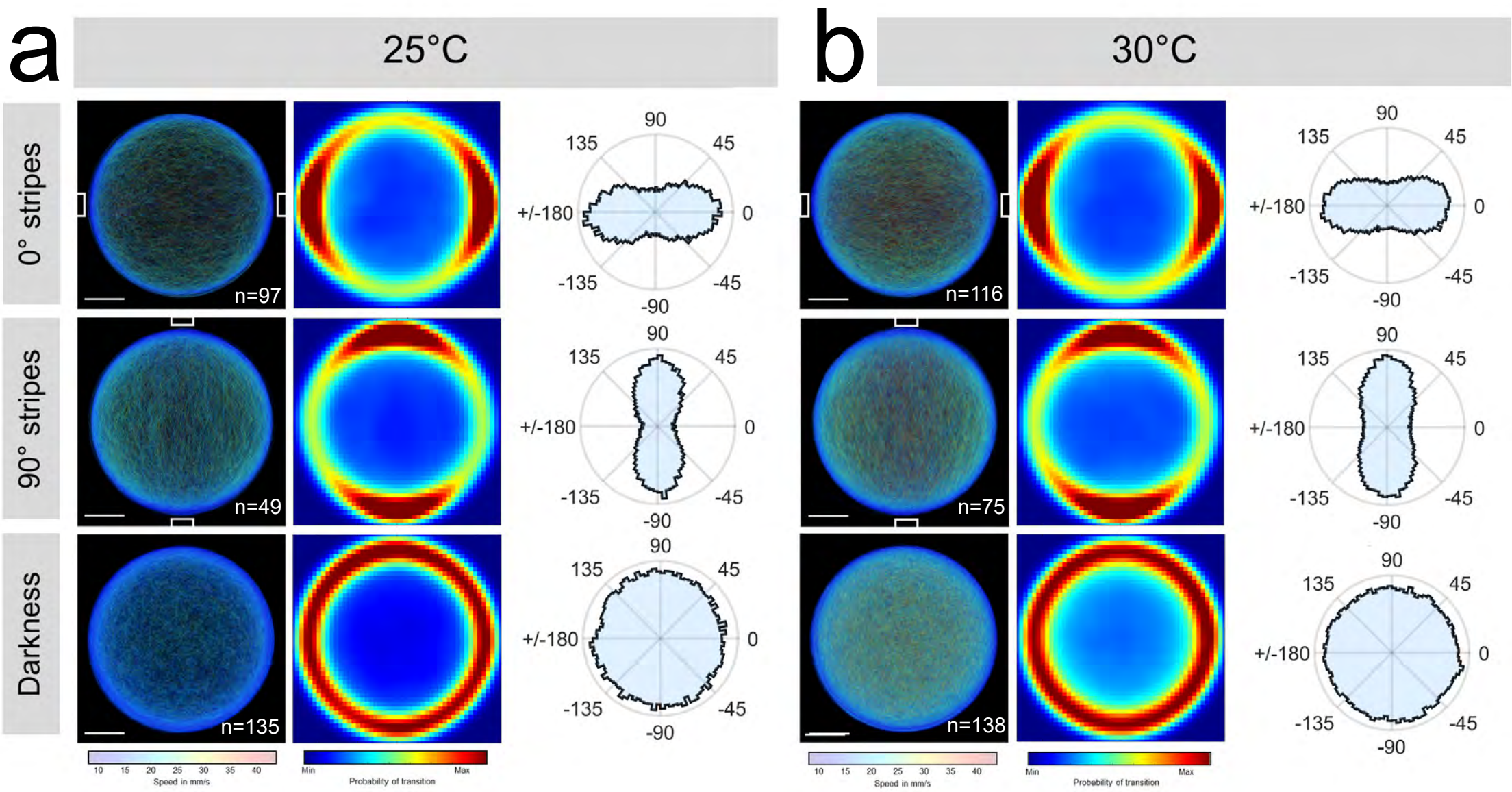

Supplemental Fig. S5: Preliminary data of a fly group (TopBanana) illustrating orientational responses. Flies walk between the 2 stripes and show randomly distributed headings in darkness, independent of temperature. **a** Velocity- (left, transparency added to tracks), transition- (middle), and angular plots (right, angles from moving periods only, non-axial) for vertical stripes positioned at 0° (top), 90° (middle) or in complete darkness (bottom), respectively for all tested flies at 25°C. Scale bar = 10mm. **b**) Same as **a**) but at 30°C. Fly numbers are indicated in the velocity plots.

Supplemental figure S6:

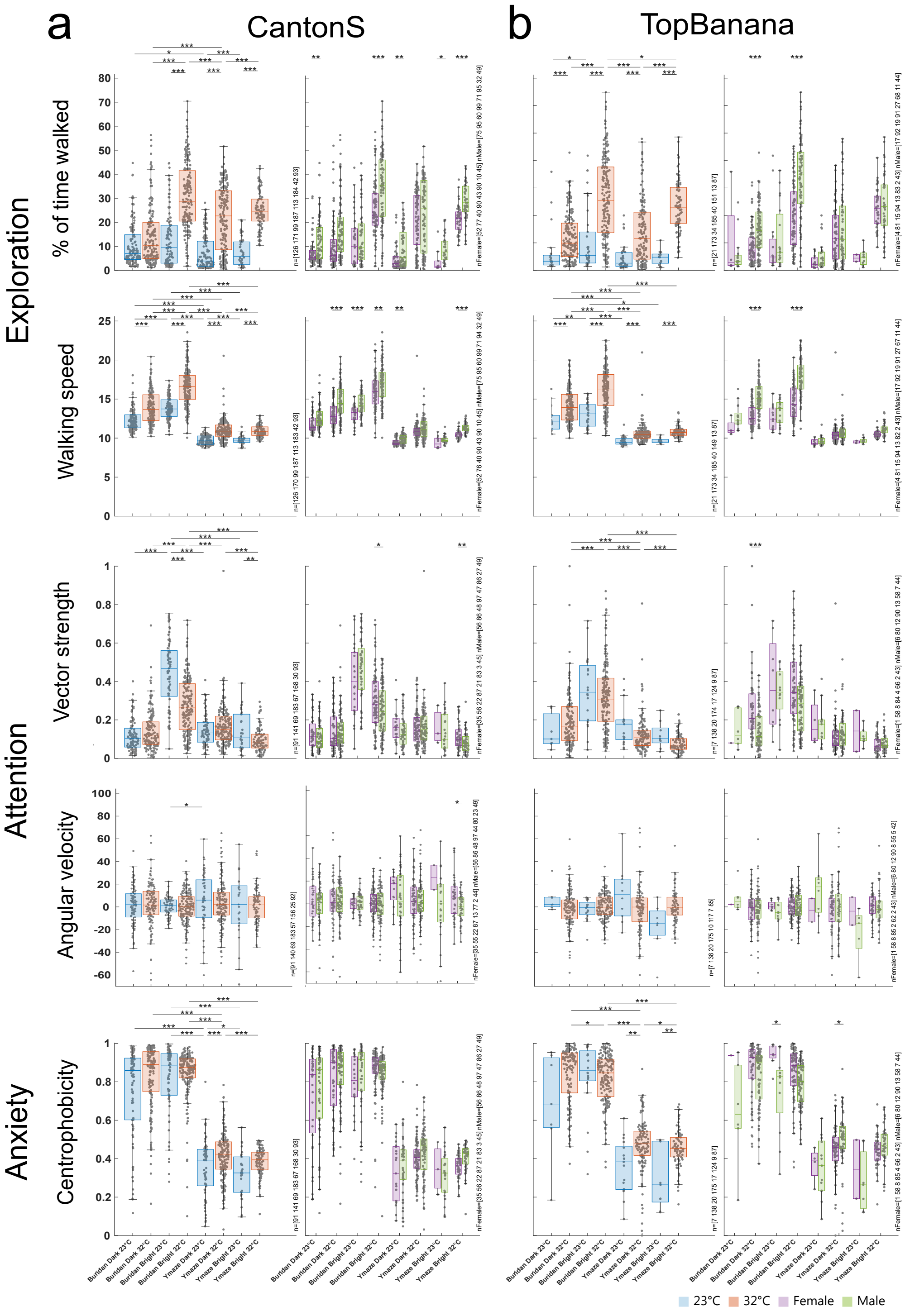

Supplemental Fig. S6: Sex- and genotype-specific group responses over varying temperature, illumination and arena shape in walking flies. **a** Boxplots illustrating key behavioral parameters for the whole tested CantonS group (left, blue=23°C, red=32°C) and separately for females/males (green/magenta) over varying temperature, illumination and arena shape. Animal numbers are indicated next to each plot. **b** Same as **a**, but for all tested TopBanana flies.

Supplemental figure S7:

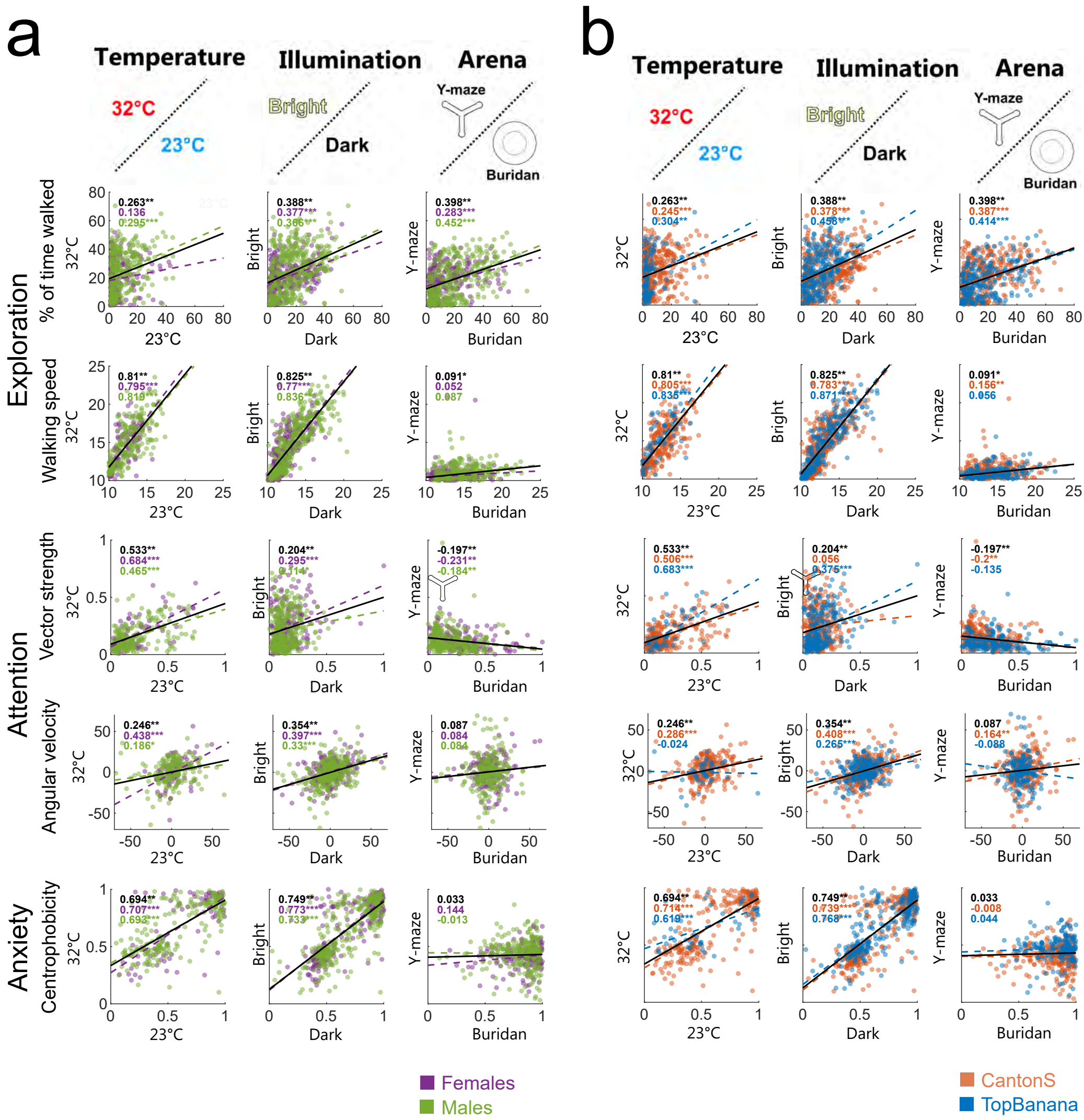

Supplemental Fig. S7: Sex- and genotype-specific differences based on the influence of temperature, illumination, and arena shape on the persistence of individual traits in walking flies. **a** Correlation of key behavioral parameters for females and males depending on temperature, illumination, and arena. Magenta=females, green=males. Correlation coefficients are displayed in the upper left corner of each plot. *=p<0.05, **=p<0.01, ***=p<0.001, for detailed fly numbers per experimental condition, see supplemental Fig. S6. **b** same as **a** but sorted by genotype (red=CantonS, blue=TopBanana).

Supplemental figure S8:

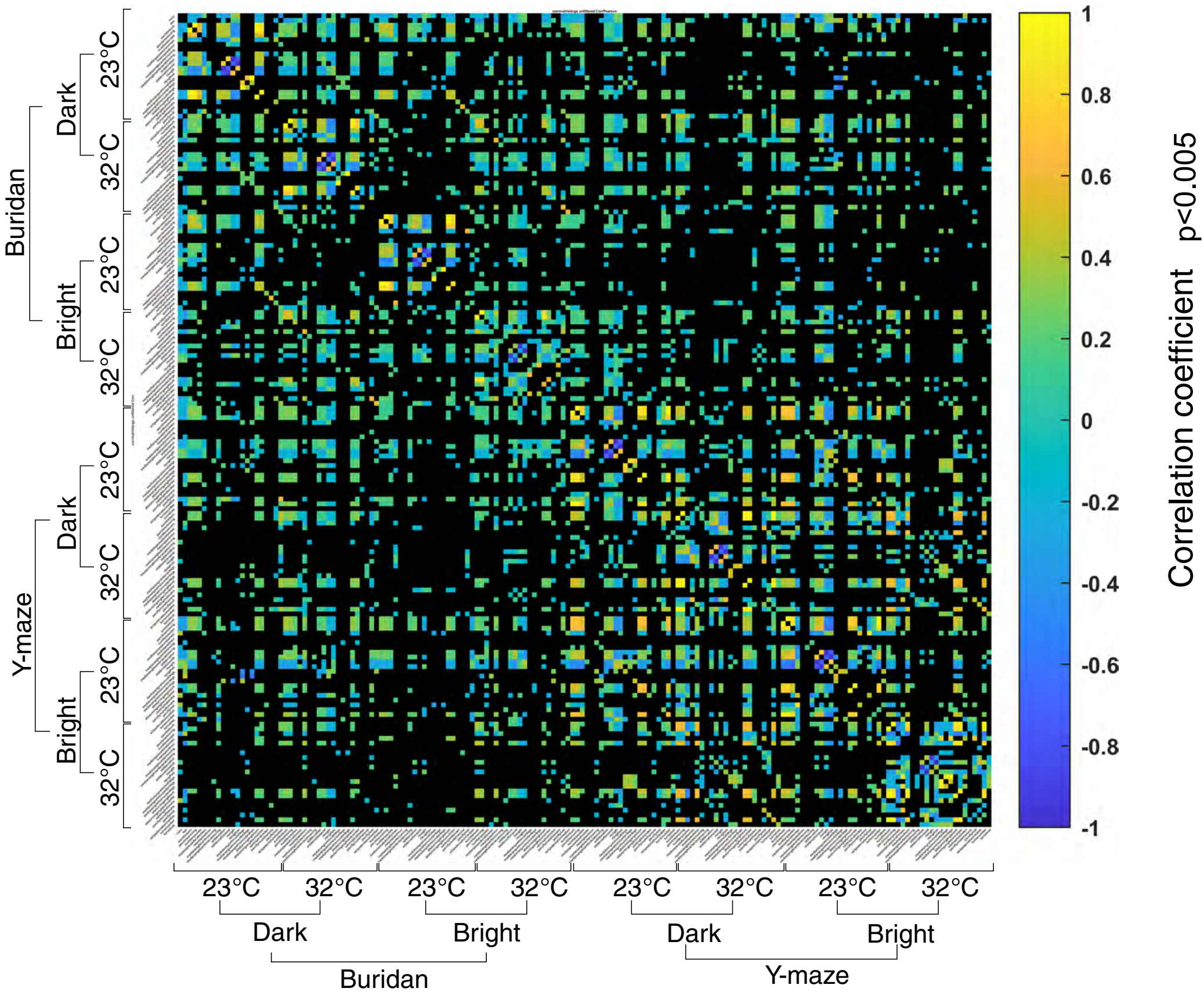

Supplemental Fig. S8: Complete correlation matrix across all behavioral parameters and contexts. Correlation coefficients with $p<0.05$ are color coded. A high resolution version of the data can be found under https://github.com/LinneweberLab/Mathejczyk_2024_eLife_Individuality/blob/main/S8.pdf.

Supplemental figure S9:

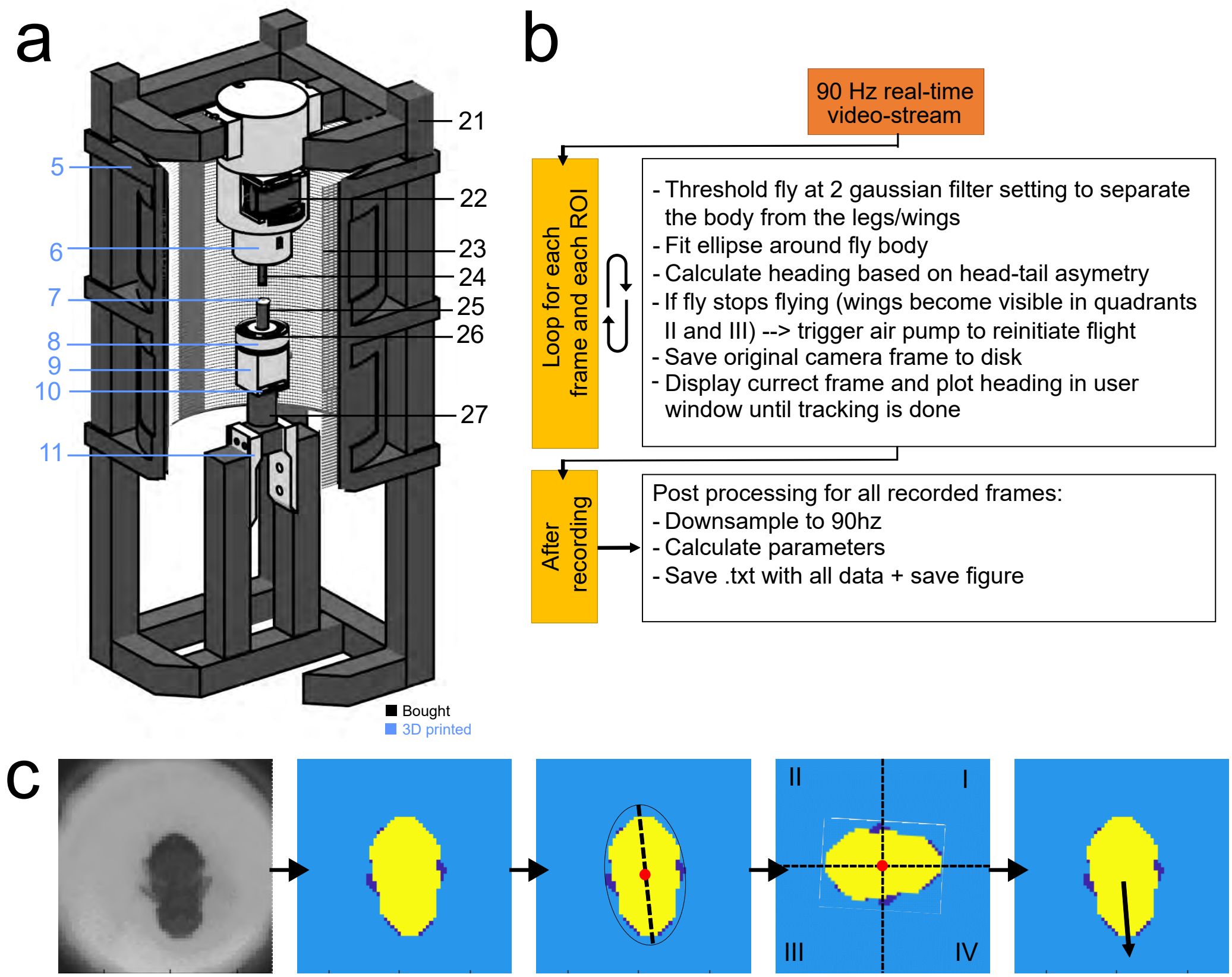

Supplemental Fig. S9: Construction of a virtual flight simulator for studying the persistence of individual traits in flying flies. **a** Overview of parts necessary for constructing the assay. Part numbers are referenced in supplemental table T2 and for 3D printed parts under github.com/LinneweberLab/Mathejczyk_2024_eLife_Individualityfor replication. Black numbers indicate off-the-shelve parts; blue numbers indicate 3D-printed parts. **b** schematic illustration of the tracking procedure. The provided MATLAB script works in real-time at ~90Hz on a 4GHz processor. The code automatically reads camera frames, computes the heading angle over time, and saves data for further analysis. **c** Illustration of the tracking procedure. The camera frame is thresholded using 2 different Gaussian filter settings to separately threshold the body (yellow) and legs/wings (dark blue). An ellipse is fitted around the thresholded body pixels, and its main axis is used to measure the distribution of body pixels within 4 virtual quadrants whose origin is the centroid of the fly. The head region can be determined because it appears smaller in the camera images than the abdominal region of the fly.

Supplemental figure S10:

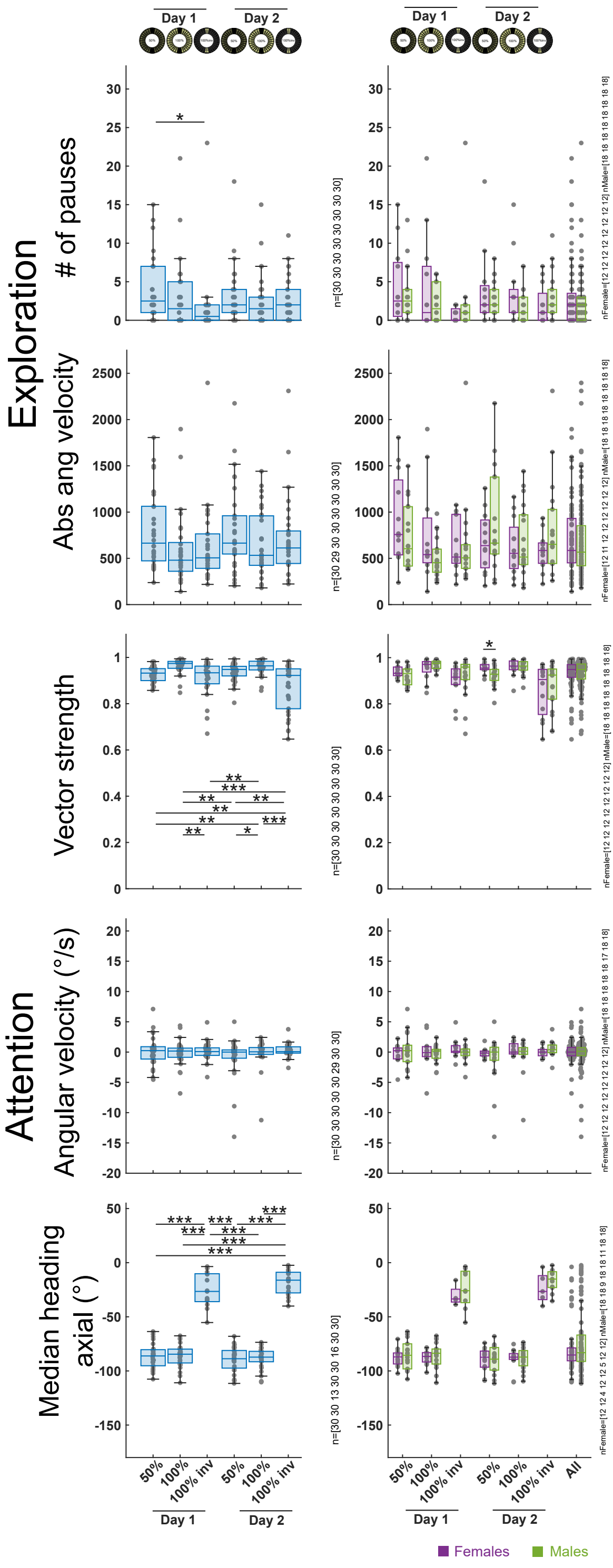

Supplemental Fig. S10: Group responses over time and different visual contrasts in flying flies. Boxplots illustrating key behavioral parameters for the whole group (blue) and separately for females/males (green/magenta) over time and varying stripe contrasts (**b**). Animal numbers are indicated next to each plot.

Supplemental figure S11:

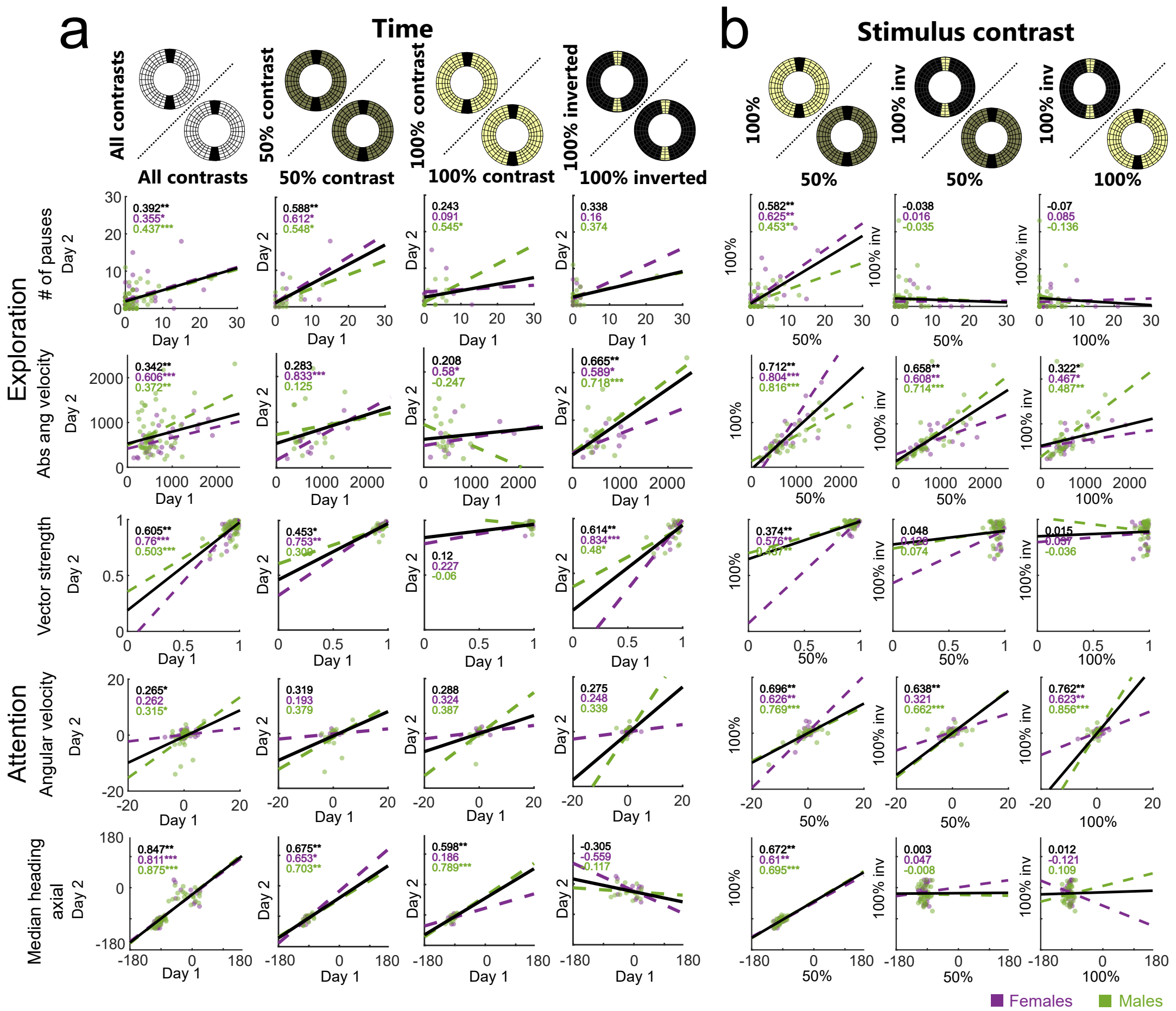

985 **Supplemental Fig. S11:** Sex-specific differences of individual traits in flying flies persist over time but
986 depend on the visual scenery. **a** Correlation of key behavioral parameters for females and males over
987 time and dependent on stimulus contrast. Magenta=females, green=males. Correlation coefficients are
988 displayed in the upper left corner of each plot. *=p<0.05, **=p<0.001, ***=p<0.0001, for detailed fly
989 numbers per experimental condition, see supplemental Fig. S10.

990

991

Supplemental figure S12:

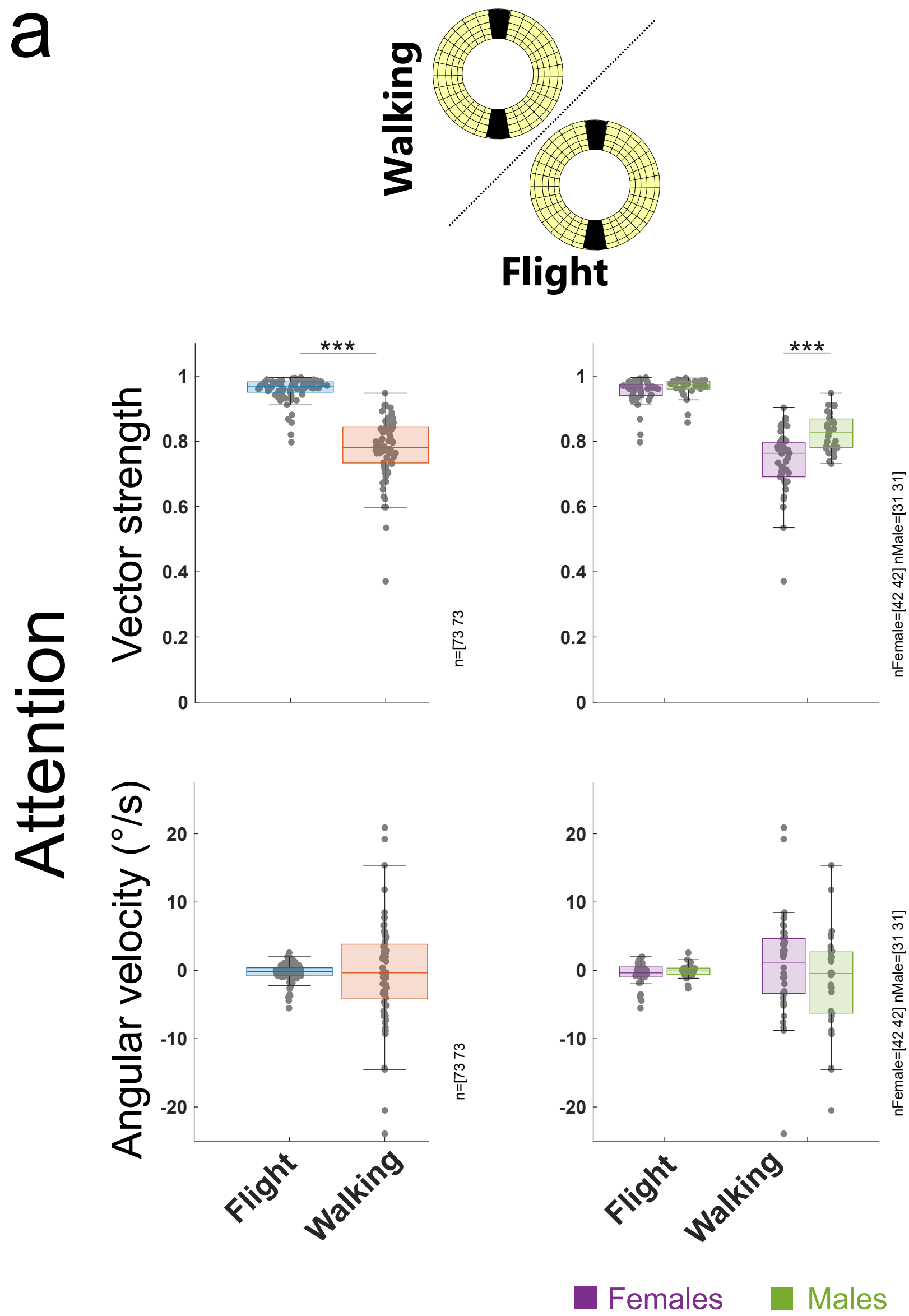

Supplemental Fig. S12: Group responses of orientational parameters across different behavioral states. Boxplots illustrating orientational parameters under different behavioral states for the whole test group (blue) and separately for females/males (green/magenta). Animal numbers are indicated next to each plot.

Supplemental figure S13:

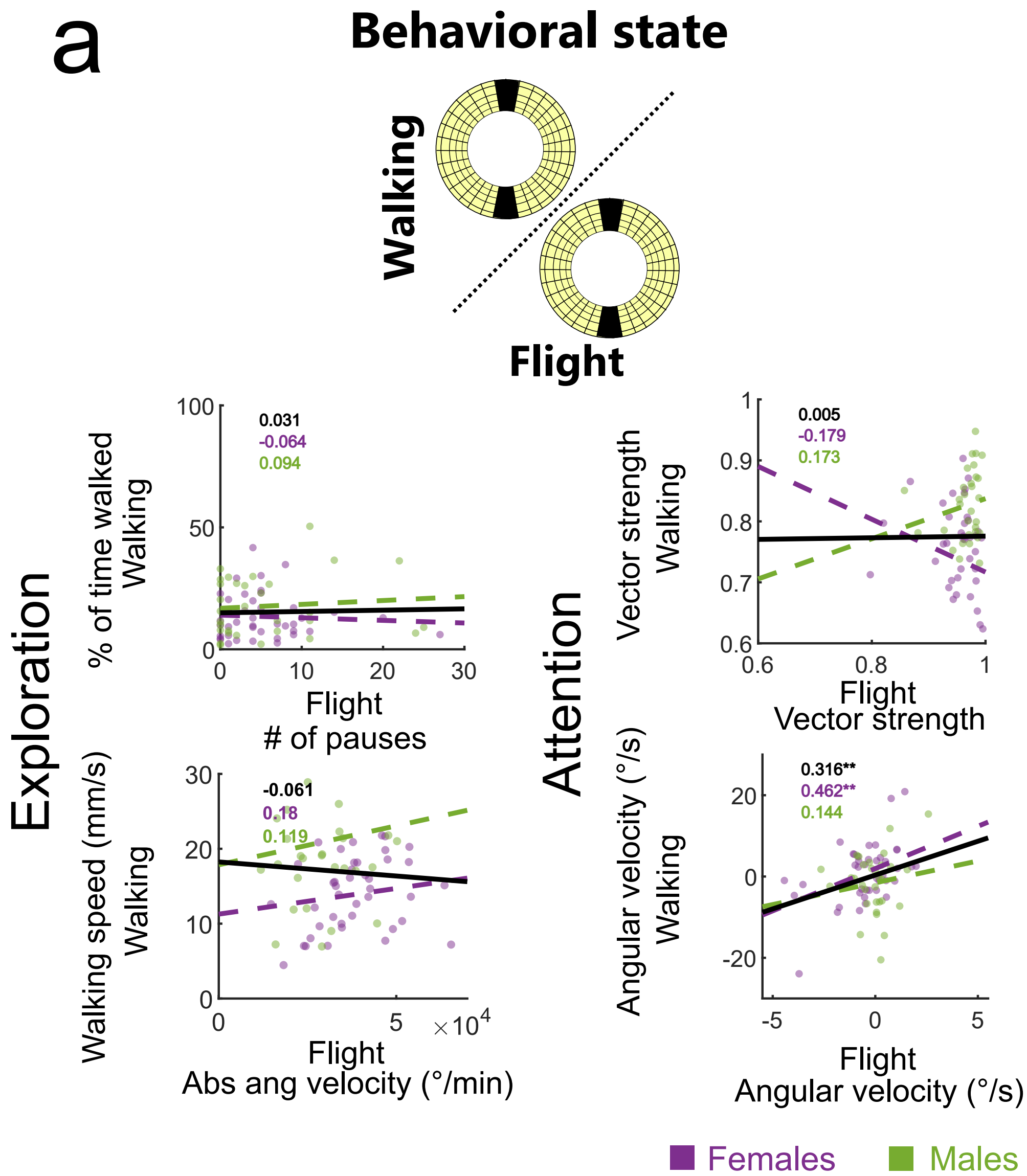

Supplemental Fig. S13: Attention persists across different behavioral states in males but not females. **a** Correlation of key behavioral parameters for females and males depending on the behavioral state. Magenta=females, green=males. Correlation coefficients are displayed in the upper left corner of each plot. *=p<0.05, **=p<0.001, ***=p<0.0001, for detailed fly numbers per experimental condition, see supplemental Fig. S12.

Supplemental table T1: Description of automatically computed output parameters

Parameter	Description
roinr	Arena number for fly identification.
sex	Male = 0, female = 1.
eucldistsum	Total distance walked in mm.
perctimemoving	% of time spent walking.
numberpauses	Number of pauses (min pause length = 1s).
medianpausedurati onsec	Median pause duration in s.
meanspeedmov	Mean walking speed in mm/s.
medianangleccenter moving	Median walking angle (heading direction) between 0° and 360° in the center region of the arena as seen from the animal.
medianangleccenter axialmoving	Median walking angle (heading direction) between 0° and 180° (axial) in the center region of the arena as seen from the animal. Axial transformation of angular data was achieved by subtracting 180 ° from all angles larger than 180 °. Axial data is more robust against cancelling -out of opposing angles in median calculations, e.g. when a fly is walking back and forth between stripes.
stddeviation	Standard deviation of angular data in ° as seen from the animal. Low angular standard deviation indicates a smaller range of chosen heading directions. Contains only data points where the animal was walking in the center region of the arena.
rlength	Resulting vector length of angular data mapped between 0° and 360°. A vector length of 0 would indicate uniform distribution of heading angles. A vector length of 1 would indicate the animl was only moving in a perfectly straight path. Contains only data points where the animal was walking in the center region of the arena.
rlengthax	Resulting vector length of angular data mapped between between 0° and 180° (axial) . A vector length of 0 would indicate uniform distribution of heading angles. A vector length of 1 would indicate the animl was only moving in a perfectly straight path. Contains only dat a points where the animal was walking in the center region of the arena. Axial data is more robust against cancelling -out of opposing angles in median calculations, e.g. when a fly is walking back and forth between stripes.
medianangvelmova lldegs	Median angular velocity (angular speed of azimuthal rotation) when walking in °/s. Median angular velocity is also a measure of handedness. Positive values indiceate right turns and negative values indicate left turns as seen from the animal.
medianangvelmovc enterdegs	Median angular velocity (angular speed of azimuthal rotation) when walking in the center region of the arena in °/s. Median angular velocity is also a measure of handedness. Positive values indiceate right turns and negative values indicate left turns as seen from the animal.
medianangvelmovo uterdegs	Median angular velocity (angular speed of azimuthal rotation) when walking in the edge region of the arena in °/s. Median angular velocity is also a measure of handedness. Positive values indiceate right turns and negative values indicate left turns as seen from the animal.
absturninganglesu m	Sum of all walking heading changes in °. Divided by distance walked this can be used as a measure for „meandering“ (heading change per mm walked in °/mm).
absturninganglesu mcenter	Sum of all walking heading changes within the center region of the arena in °. Divided by distance walked this can be used as a measure for „meandering“ (heading change per mm walked in °/mm).
centrophobindex	Centrophobicity index between 0 and 1. 0 indicates an animal being in the center area 100% of the time. 1 indicates an animal being in the edge area 100% of the time.
pecflymorethanone	% of time with more than two objects detected per arena. This parameter indicates false animal detections (e.g dust) and and is useful for validating tracking quality or finding tracking errors.
percflylost	% of time the tracker lost an animal. This parameter is useful for validating tracking quality or finding tracking errors.
stripedeviationmed ian	Applies to Buridan data. Medain angular distance to the closest (in terms of azimuthal rotation) stripe when walking in the center of the arena in °.
turnsnumber	Applies to Y -maze data. Number of turns. One turn is defined as an animal (measured at center point) walking from one Y-maze arm 3mm into another.
turnsbias	Ratio of right VS left turns. Values larger than 0.5 indicate right -handedness. Values smaller than 0.5 indicate left-handedness.

Supplemental table T2: Part list for setup replication

LED Buridan Setup		
Nr	**Description**	**Amount**
1	Flir Firefly S FFY-U3-04S2M-C + Edmund optics UC Series Fixed Focal Length Objective (8mm, Stock #33-307)	1
2	Acrylic plate white opaque matt 500 x 410 x 3 mm (30mm circular hole in center)	1
3	Clear acrylic cylinder (300mm diameter, 300mm height) + diffuser paper or satinice acrylic cylinder (300mm diameter, 300mm height)	1
4	Fluorscent tubes (Osram, L 40w, 640C circular cool white) + Osram QT-M 1626–42 controller for AC flicker rate >1kHz	4
5	Aluminium profiles black (45 x 45 mm) P45N10LS www.aluprofile24.de:	
	400mm + thread M12 (min 100mm) profile	4
	480mm profile	2
	485mm profile	1
	+ Construction accessories www.aluprofile24.de:	
	Wi45x45 angle	10
	IWiN10 angle	20
	BuMuM8 nut screw	20
	FußD40DG m12x100 feet	4
	+ BitFenix Spectre PRO 230 mm mounted between aluminium rails on 2 opposing sides of the setup for cooling the LED matrix	8
6	6x RGB LED matrix (128 x 64 pixel) www.ledall.de 1x Hdmi controller Novastar mctrl 660 pro + 1x Novastar A8S receiving card 6x	1
	+ Famotec locating ring 3mm inner diameter (EAN: 4053199955619) + grub screw M3 x 20mm for fixing LED matrix to the LED cylinder	150
7	Transparent acrylic dome 120mm diameter (www.architekturbedarf.de) coated with Sigmacote on the inside	1
8	PLEXIGLAS® WH10 DC white snow satinice disk 119 x 119 x 10 mm + 850nm LED strip wrapped around edge for backlight illumintaion	1
9	Acrylic plate white opaque matt 500 x 500 x 3 mm (120mm circular hole in center)	1
10	PLEXIGLAS® WH10 DC white snow satinice 500 x 500 x 3 mm	1
11	PLEXIGLAS® WH10 DC white snow satinice disk 119 x 119 x 10 mm + 850nm LED strip (www.ledxess.de) wrapped around edge for backlight illumintaion	1
12	PLEXIGLAS® WH10 DC white snow satinice 500 x 500 x 10 mm (300mm circular hole in center)	2
IndyTrax Setup		
Nr	**Description**	**Amount**
13	120x12mm EEC0381B1-000U-A99 Sunon	4
14	880nm infrared backlight https://www.amazon.de/LED-Lichttherapie-Dunkelrotes-Infrarot-LED-Lichttherapie-Panel-Hautverj%C3%BCngung-Druckentlastung/dp/B07ZQ	1
15	Server cabinet https://www.serverschrank24.de/15-he-serverschrank-wandgehause-mit-glastur-bxtxh-600-x-450-x-820-mm.html	1
16	Translucent acrylic cylinder https://www.kus-kunststofftechnik.de/plexiglas-rohr/plexiglasxt-satiniert-o-60-mm-laenge-waehlbar-von-100-bis-1400-mm/	25
16	Electroluminescent foil A7 white	50
16	Transparent dome 50mm https://www.dekoweltcreativ.de/acrylkugel-transparent-teilbar-stueck/p-3330.html	25
16	Plexiglas GS white 70% 3mm WH10 49mm diameter https://www.plattenzuschnitt24.de/Plexiglas-GS-weiss-WH10-GT-3mm.html	50
17	19" drawer https://www.it-budget.de/19-Fachboden-ausziehbar-Vollauszug-Tragkraft-30-kg-350-mm-schwarz	2
18	Camera Point Grey BFLY-PGE-23S6C-C mounted on Rack chassis 24563-194nVent – Schroff	1
18	Objective LM8HC3HOLE 1" 8mm/F1.4	1
19	BitFenix Spectre PRO 230 mm	2
20	Carbon heater https://thermowelt.de/Artikel/carbonheater1-1GN-220V.html	1
Controllers	Humidity controller TXG top-messtechnik.com TMT-HC-210 controlls 40x40mm Sunon EE40101S1-1000U-999 Axiallüfter 12 V/DC placed on (4)	1
	PID temperature controller pohltechnic.com RT4-121-Tr21Sd controlls (20)	1
	VOLTCRAFT LSP-1165 for controlling IR LED panel (14) and fans (18, 19)	2
	TT COMMANDER FT for cooling down enclosure, if necessary (controlls enclosure fans (13))	1
	Inverter https://www.el-light.shop/epages/17778431.sf/de_DE/?ObjectPath=/Shops/17778431/Products/InF1S150 controlls el-foil (16) brightness	1
LED flight simulator		
Nr	**Description**	**Amount**
21	Aluminium profiles black (30 x 30 mm) P30N8 www.aluprofile24.de:	
	600mm profile	4
	165mm profile	10
	200mm profile	2
	+ Construction accessories www.aluprofile24.de:	
	PADK30N8B cap	4
	IWIN8B angle	25
	BuMuM6 nut screw	10
	WI30N8B	10
	HaKoM6 (12mm)	20
22	optional servo motor for dorsal stimulus presentation (Dynamixel MX-12W) + ball bearing 6811-ZZ (www.kugellager-express.de)	1
23	4x RGB LED matrix (128 x 64 pixel) www.ledall.de + 1x Hdmi controller Novastar mctrl 660 pro + 1x Novastar A8S receiving card	1
	+ Famotec locating ring 3mm inner diameter (EAN: 4053199955619) + grub screw M3 x 20mm for fixing LED matrix to the LED cylinder	150
24	Neodynium cylinder magnet (5mm diameter, 20mm height) + white plastic cap + 1mm diameter v-shaped sapphire bearing in center for friction reduction	1
25	Neodynium ring magnet (10mm diameter, 5mm height, inner diameter 5mm) + white plastic cap	1
26	850nm near infrared LED array (https://www.amazon.de/POFET-Infrarot-IR-LED-850-nm-Platinenmodul-f%C3%BCr-das-Kamera%C3%Bcberwachungssystem)	1
27	Flir Firefly S FFY-U3-04S2M-C + Edmund optics UC Series Fixed Focal Length Objective (12mm, Stock #33-307)	1
Air puffs	Arduino UNO Rev3 + relais module + Schego membrane pump 300l/h	1

Walking								
Name	**Estimate**	**SE**	**tStat**	**DF**	**pValue**	**Lower**	**Upper**	**Trait**
(Intercept)	-36.0989	1.703036	-21.1968	2977	5.45E-93	-39.4381	-32.7596	% of time walked
Day	0.114762	0.525089	0.218558	2977	0.827009	-0.91481	1.144337	% of time walked
Temp_C	1.641446	0.045068	36.4213	2977	1.57E-240	1.553078	1.729814	% of time walked
StripeNum	2.287736	0.401177	5.702555	2977	1.30E-08	1.501123	3.074349	% of time walked
Illumination	4.202395	0.644612	6.519264	2977	8.27E-11	2.938465	5.466325	% of time walked
ArenaType	-0.18729	0.782171	-0.23945	2977	0.81077	-1.72094	1.346356	% of time walked
(Intercept)	8.535013	0.29851	28.59203	2906	1.19E-158	7.9497	9.120327	Walking speed (in mm/s)
Day	0.708806	0.085192	8.32006	2906	1.33E-16	0.541762	0.87585	Walking speed (in mm/s)
Temp_C	0.228039	0.008173	27.89993	2906	5.54E-152	0.212013	0.244066	Walking speed (in mm/s)
StripeNum	0.582187	0.071393	8.154717	2906	5.15E-16	0.442202	0.722173	Walking speed (in mm/s)
Illumination	0.57637	0.114911	5.015818	2906	5.60E-07	0.351056	0.801685	Walking speed (in mm/s)
ArenaType	-3.52742	0.130363	-27.0584	2906	5.31E-144	-3.78303	-3.2718	Walking speed (in mm/s)
(Intercept)	0.740154	0.033723	21.94792	2660	2.87E-98	0.674028	0.80628	Vector strength
Day	0.039671	0.008519	4.656816	2660	3.37E-06	0.022967	0.056375	Vector strength
Temp_C	-0.02178	0.000899	-24.2139	2660	3.19E-117	-0.02354	-0.02002	Vector strength
StripeNum	0.115137	0.007552	15.24591	2660	2.22E-50	0.100329	0.129946	Vector strength
Illumination	-0.04424	0.011957	-3.70031	2660	0.00022	-0.06769	-0.0208	Vector strength
ArenaType	0.000995	0.013366	0.074413	2660	0.940687	-0.02521	0.027204	Vector strength
(Intercept)	6.076388	4.194318	1.448719	2093	0.147566	-2.14908	14.30186	Angularvelocity (in °/s)
Day	0.724146	0.969316	0.747069	2093	0.455106	-1.17678	2.625069	Angularvelocity (in °/s)
Temp_C	-0.14832	0.121757	-1.21813	2093	0.223311	-0.38709	0.090461	Angularvelocity (in °/s)
StripeNum	0.153049	0.930464	0.164487	2093	0.869364	-1.67168	1.97778	Angularvelocity (in °/s)
Illumination	-1.77591	1.572772	-1.12916	2093	0.258959	-4.86027	1.308446	Angularvelocity (in °/s)
ArenaType	0.471883	1.721123	0.274171	2093	0.78398	-2.90341	3.847173	Angularvelocity (in °/s)
(Intercept)	1.016901	0.038389	26.48924	2981	4.94E-139	0.941629	1.092173	Centrophobicity
Day	-0.02827	0.009991	-2.82914	2981	0.004699	-0.04786	-0.00868	Centrophobicity
Temp_C	0.0064	0.001061	6.031474	2981	1.82E-09	0.00432	0.008481	Centrophobicity
StripeNum	0.023118	0.008831	2.617863	2981	0.008893	0.005803	0.040433	Centrophobicity
Illumination	-0.05418	0.014117	-3.83793	2981	0.000127	-0.08186	-0.0265	Centrophobicity
ArenaType	-0.33056	0.015574	-21.2253	2981	3.16E-93	-0.3611	-0.30002	Centrophobicity
Flight								
Name	**Estimate**	**SE**	**tStat**	**DF**	**pValue**	**Lower**	**Upper**	**Trait**
(Intercept)	1.405556	1.082089	1.298927	177	0.195658	-0.7299	3.541013	Number of pauses
Day	-0.05556	0.519965	-0.10684	177	0.915033	-1.08168	0.970573	Number of pauses
Contrast	0.725	0.318412	2.276924	177	0.023988	0.096627	1.353373	Number of pauses
(Intercept)	585.0846	125.6295	4.657222	177	6.27E-06	337.1601	833.0091	Abs ang velocity sum (in °/min)
Day	5.265697	57.14176	0.092151	177	0.926682	-107.501	118.0325	Abs ang velocity sum (in °/min)
Contrast	61.74883	34.99204	1.764654	177	0.079347	-7.30646	130.8041	Abs ang velocity sum (in °/min)
(Intercept)	0.9028	0.019721	45.77796	177	4.87E-100	0.863881	0.94172	Vector strength
Day	-0.01242	0.009861	-1.25997	177	0.209338	-0.03188	0.007035	Vector strength
Contrast	0.021463	0.006038	3.554403	177	0.000486	0.009546	0.033379	Vector strength
(Intercept)	0.703611	0.741426	0.948997	177	0.343916	-0.75956	2.166784	Angular velocity (in °/s)
Day	-0.51914	0.329735	-1.57442	177	0.117176	-1.16986	0.131577	Angular velocity (in °/s)
Contrast	-0.07577	0.20192	-0.37525	177	0.70792	-0.47425	0.32271	Angular velocity (in °/s)
(Intercept)	218.6298	8.189625	26.69595	177	5.80E-64	202.468	234.7917	Heading (in °)
Day	-4.84511	4.094813	-1.18323	177	0.238304	-12.926	3.235827	Heading (in °)
Contrast	-44.6257	2.50755	-17.7965	177	2.79E-41	-49.5742	-39.6772	Heading (in °)

Supplemental table T3: Fixed-effects summary from hierarchical linear mixed-model analysis for all behavioral traits. For each behavioral trait, the model included environmental context variables as fixed effects and fly identity (ID) as a random intercept. Name: fixed-effect terms. Estimate: estimated effect size on the respective trait (in trait units). SE: standard error of estimate. DF: degrees of freedom used for testing significance. tStat: t-statistic. p-value: p-value. Lower/upper: bound of the 95% confidence interval for the effect estimate. Trait: behavioral trait.

References

Andrew Sih, Alison M Bell, J Chadwick Johnson, & Robert E Ziemba. (2004). Behavioral Syndromes: An Integrative Overview. *The Quarterly Review of Biology*, *79*(3), 241-277. https://doi.org/10.1086/422893

Ayroles, J. F., Buchanan, S. M., O'Leary, C., Skutt-Kakaria, K., Grenier, J. K., Clark, A. G., Hartl, D. L., & de Bivort, B. L. (2015). Behavioral idiosyncrasy reveals genetic control of phenotypic variability. *Proceedings of the National Academy of Sciences*, *112*(21), 6706-6711. https://doi.org/doi:10.1073/pnas.1503830112

Baines, R. A., Uhler, J. P., Thompson, A., Sweeney, S. T., & Bate, M. (2001). Altered Electrical Properties in DrosophilaNeurons Developing without Synaptic Transmission. *The Journal of Neuroscience*, *21*(5), 1523-1531. https://doi.org/10.1523/jneurosci.21-05-01523.2001

Bell, A. M., Hankison, S. J., & Laskowski, K. L. (2009). The repeatability of behaviour: a meta-analysis. *Animal Behaviour*, *77*(4), 771-783. https://doi.org/https://doi.org/10.1016/j.anbehav.2008.12.022

Berens, P. (2009). CircStat: A MATLAB Toolbox for Circular Statistics. *2009*, *31*(10), 21. https://doi.org/10.18637/jss.v031.i10

Boissy, A., & Bouissou, M. F. (1995). Assessment of individual differences in behavioural reactions of heifers exposed to various fear-eliciting situations. *Applied Animal Behaviour Science*, *46*(1), 17-31. https://doi.org/https://doi.org/10.1016/0168-1591(95)00633-8

Branson, K., Robie, A. A., Bender, J., Perona, P., & Dickinson, M. H. (2009). High-throughput ethomics in large groups of Drosophila. *Nat Methods*, *6*(6), 451-457. https://doi.org/10.1038/nmeth.1328

Briffa, M., & Greenaway, J. (2011). High In Situ Repeatability of Behaviour Indicates Animal Personality in the Beadlet Anemone Actinia equina (Cnidaria). *PLoS One*, *6*(7), e21963. https://doi.org/10.1371/journal.pone.0021963

Briffa, M., Rundle, S. D., & Fryer, A. (2008). Comparing the strength of behavioural plasticity and consistency across situations: animal personalities in the hermit crab Pagurus bernhardus. *Proc Biol Sci*, *275*(1640), 1305-1311. https://doi.org/10.1098/rspb.2008.0025

Buchanan, S. M., Kain, J. S., & de Bivort, B. L. (2015). Neuronal control of locomotor handedness in Drosophila. *Proc Natl Acad Sci U S A*, *112*(21), 6700-6705. https://doi.org/10.1073/pnas.1500804112

Bülthoff, H., Götz, K. G., & Herre, M. (1982). Recurrent inversion of visual orientation in the walking fly,Drosophila melanogaster. *Journal of comparative physiology*, *148*(4), 471-481. https://doi.org/10.1007/BF00619785

Carter, M., & Shieh, J. (2015). Chapter 2 - Animal Behavior. In M. Carter & J. Shieh (Eds.), *Guide to Research Techniques in Neuroscience (Second Edition)* (pp. 39-71). Academic Press. https://doi.org/https://doi.org/10.1016/B978-0-12-800511-8.00002-2

Coleman, K., & Wilson, D. S. (1998). Shyness and boldness in pumpkinseed sunfish: individual differences are context-specific. *Animal Behaviour*, *56*(4), 927-936. https://doi.org/https://doi.org/10.1006/anbe.1998.0852

Colomb, J., Reiter, L., Blaszkiewicz, J., Wessnitzer, J., & Brembs, B. (2012). Open source tracking and analysis of adult Drosophila locomotion in Buridan's paradigm with and without visual targets. *PLoS One*, *7*(8), e42247. https://doi.org/10.1371/journal.pone.0042247

Costa, P. T., Jr., & McCrae, R. R. (1988). Personality in adulthood: a six-year longitudinal study of self-reports and spouse ratings on the NEO Personality Inventory. *J Pers Soc Psychol*, *54*(5), 853-863. https://doi.org/10.1037//0022-3514.54.5.853

Crabbe, J. C., Wahlsten, D., & Dudek, B. C. (1999). Genetics of Mouse Behavior: Interactions with Laboratory Environment. *Science*, *284*(5420), 1670-1672. https://doi.org/doi:10.1126/science.284.5420.1670

D'Eath, R., & Burn, C. (2002). INDIVIDUAL DIFFERENCES IN BEHAVIOUR: A TEST OF 'COPING STYLE' DOES NOT PREDICT RESIDENT-INTRUDER AGGRESSIVENESS IN PIGS. *Behaviour*, *139*(9), 1175-1194. https://doi.org/https://doi.org/10.1163/15685390260437326

Dall, S. R. X., Houston, A. I., & McNamara, J. M. (2004). The behavioural ecology of personality: consistent individual differences from an adaptive perspective. *Ecology Letters*, *7*(8), 734-739. https://doi.org/https://doi.org/10.1111/j.1461-0248.2004.00618.x

Diener, E., & Larsen, R. J. (1984). Temporal stability and cross-situational consistency of affective, behavioral, and cognitive responses. *J Pers Soc Psychol*, *47*(4), 871-883. https://doi.org/10.1037//0022-3514.47.4.871

Dingemanse, N. J., & Dochtermann, N. A. (2013). Quantifying individual variation in behaviour: mixed-effect modelling approaches. *Journal of Animal Ecology*, *82*(1), 39-54. https://doi.org/https://doi.org/10.1111/1365-2656.12013

Dorkenwald, S., Matsliah, A., Sterling, A. R., Schlegel, P., Yu, S.-c., McKellar, C. E., Lin, A., Costa, M., Eichler, K., Yin, Y., Silversmith, W., Schneider-Mizell, C., Jordan, C. S., Brittain, D., Halageri, A., Kuehner, K., Ogedengbe, O., Morey, R., Gager, J.,…The FlyWire, C. (2024). Neuronal wiring diagram of an adult brain. *Nature*, *634*(8032), 124-138. https://doi.org/10.1038/s41586-024-07558-y

Fleeson, W. (2001). Toward a structure- and process-integrated view of personality: traits as density distribution of states. *J Pers Soc Psychol*, *80*(6), 1011-1027. https://www.ncbi.nlm.nih.gov/pubmed/11414368

Freund, J., Brandmaier, A. M., Lewejohann, L., Kirste, I., Kritzler, M., Krüger, A., Sachser, N., Lindenberger, U., & Kempermann, G. (2013). Emergence of Individuality in Genetically Identical Mice. *Science*, *340*(6133), 756-759. https://doi.org/doi:10.1126/science.1235294

Galton, F. (1875). The history of twins, as a criterion of the relative powers of nature and nurture. *Fraser's Magazine*, *12*(71), 566-576.

Geissmann, Q., Garcia Rodriguez, L., Beckwith, E. J., French, A. S., Jamasb, A. R., & Gilestro, G. F. (2017). Ethoscopes: An open platform for high-throughput ethomics. *PLOS Biology*, *15*(10), e2003026. https://doi.org/10.1371/journal.pbio.2003026

Gibert, J. P., Chelini, M.-C., Rosenthal, M. F., & DeLong, J. P. (2016). Crossing regimes of temperature dependence in animal movement. *Global Change Biology*, *22*(5), 1722-1736. https://doi.org/https://doi.org/10.1111/gcb.13245

Gosling, S. D. (2008). Personality in Non-human Animals. *Social and Personality Psychology Compass*, *2*(2), 985-1001. https://doi.org/https://doi.org/10.1111/j.1751-9004.2008.00087.x

Götz, K. G. (1980). Visual Guidance in Drosophila. In O. Siddiqi, P. Babu, L. M. Hall, & J. C. Hall (Eds.), *Development and Neurobiology of Drosophila* (pp. 391-407). Springer US. https://doi.org/10.1007/978-1-4684-7968-3_28

Hamada, F. N., Rosenzweig, M., Kang, K., Pulver, S. R., Ghezzi, A., Jegla, T. J., & Garrity, P. A. (2008). An internal thermal sensor controlling temperature preference in Drosophila. *Nature*, *454*(7201), 217-220. https://doi.org/10.1038/nature07001

Han, R., Wei, T.-M., Tseng, S.-C., & Lo, C.-C. (2021). Characterizing approach behavior of Drosophila melanogaster in Buridan's paradigm. *PLoS One*, *16*(1), e0245990. https://doi.org/10.1371/journal.pone.0245990

Hartshorne, H., & May, M. A. (1930). *Studies in the Nature of Character: Studies in deceit*. McMillian. https://books.google.de/books?id=cZi7xwEACAAJ

Hassan, B. A., Bermingham, N. A., He, Y., Sun, Y., Jan, Y. N., Zoghbi, H. Y., & Bellen, H. J. (2000). atonal regulates neurite arborization but does not act as a proneural gene in the Drosophila brain. *Neuron*, *25*(3), 549-561. https://doi.org/10.1016/s0896-6273(00)81059-4

Herborn, K. A., Macleod, R., Miles, W. T. S., Schofield, A. N. B., Alexander, L., & Arnold, K. E. (2010). Personality in captivity reflects personality in the wild. *Animal Behaviour*, *79*(4), 835-843. https://doi.org/10.1016/j.anbehav.2009.12.026

Hirsch, J. (1959). Studies in experimental behavior genetics. II. Individual differences in geotaxis as a function of chromosome variations in synthesized Drosophila populations. *J Comp Physiol Psychol*, *52*(3), 304-308. https://doi.org/10.1037/h0043498

Hirsch, J., & Boudreau, J. C. (1958). Studies in experimental behavior genetics. I. The heritability of phototaxis in a population of Drosophila melanogaster. *J Comp Physiol Psychol*, *51*(6), 647-651. https://doi.org/10.1037/h0039498

Honegger, K., & de Bivort, B. (2018). Stochasticity, individuality and behavior. *Curr Biol*, *28*(1), R8-R12. https://doi.org/10.1016/j.cub.2017.11.058

Honegger, K. S., Smith, M. A.-Y., Churgin, M. A., Turner, G. C., & de Bivort, B. L. (2020). Idiosyncratic neural coding and neuromodulation of olfactory individuality in Drosophila. *Proceedings of the National Academy of Sciences*, *117*(38), 23292-23297. https://doi.org/doi:10.1073/pnas.1901623116

Jiang, H., Hanna, E., Gatto, C. L., Page, T. L., Bhuva, B., & Broadie, K. (2016). A fully automated Drosophila olfactory classical conditioning and testing system for behavioral learning and memory assessment. *Journal of Neuroscience Methods*, *261*, 62-74. https://doi.org/https://doi.org/10.1016/j.jneumeth.2015.11.030

Kahsai, L., & Zars, T. (2011). Learning and Memory in Drosophila: Behavior, Genetics, and Neural Systems. In N. Atkinson (Ed.), *International Review of Neurobiology* (Vol. 99, pp. 139-167). Academic Press. https://doi.org/https://doi.org/10.1016/B978-0-12-387003-2.00006-9

Kain, J. S., Stokes, C., & de Bivort, B. L. (2012). Phototactic personality in fruit flies and its suppression by serotonin and white. *Proceedings of the National Academy of Sciences*, *109*(48), 19834-19839. https://doi.org/doi:10.1073/pnas.1211988109

Kiral, F. R., Linneweber, G. A., Mathejczyk, T., Georgiev, S. V., Wernet, M. F., Hassan, B. A., von Kleist, M., & Hiesinger, P. R. (2020). Autophagy-dependent filopodial kinetics restrict synaptic partner choice during Drosophila brain wiring. *Nature Communications*, *11*(1), 1325. https://doi.org/10.1038/s41467-020-14781-4

Klapoetke, N. C., Murata, Y., Kim, S. S., Pulver, S. R., Birdsey-Benson, A., Cho, Y. K., Morimoto, T. K., Chuong, A. S., Carpenter, E. J., Tian, Z., Wang, J., Xie, Y., Yan, Z., Zhang, Y., Chow, B. Y., Surek, B., Melkonian, M., Jayaraman, V., Constantine-Paton, M.,…Boyden, E. S. (2014). Independent optical excitation of distinct neural populations. *Nat Methods*, *11*(3), 338-346. https://doi.org/10.1038/nmeth.2836

Konopka, R. J., & Benzer, S. (1971). Clock Mutants of Drosophila melanogaster. *Proceedings of the National Academy of Sciences*, *68*(9), 2112-2116. https://doi.org/10.1073/pnas.68.9.2112

Kralj-Fišer, S., Scheiber, I. B. R., Blejec, A., Moestl, E., & Kotrschal, K. (2007). Individualities in a flock of free-roaming greylag geese: Behavioral and physiological consistency over time and across situations. *Hormones and Behavior*, *51*(2), 239-248. https://doi.org/https://doi.org/10.1016/j.yhbeh.2006.10.006

Lapiedra, O., Schoener, T. W., Leal, M., Losos, J. B., & Kolbe, J. J. (2018). Predator-driven natural selection on risk-taking behavior in anole lizards. *Science*, *360*(6392), 1017-1020. https://doi.org/doi:10.1126/science.aap9289

Linneweber, G. A., Andriatsilavo, M., Dutta, S. B., Bengochea, M., Hellbruegge, L., Liu, G., Ejsmont, R. K., Straw, A. D., Wernet, M., Hiesinger, P. R., & Hassan, B. A. (2020). A neurodevelopmental origin of behavioral individuality in the Drosophila visual system. *Science*, *367*(6482), 1112-1119. https://doi.org/10.1126/science.aaw7182

Lithgow, G. J., Driscoll, M., & Phillips, P. (2017). A long journey to reproducible results. *Nature*, *548*(7668), 387-388. https://doi.org/10.1038/548387a

Luan, H., Lemon, W. C., Peabody, N. C., Pohl, J. B., Zelensky, P. K., Wang, D., Nitabach, M. N., Holmes, T. C., & White, B. H. (2006). Functional dissection of a neuronal network required for cuticle tanning and wing expansion in Drosophila. *J Neurosci*, *26*(2), 573-584. https://doi.org/10.1523/JNEUROSCI.3916-05.2006

Luan, H., Peabody, N. C., Vinson, C. R., & White, B. H. (2006). Refined spatial manipulation of neuronal function by combinatorial restriction of transgene expression. *Neuron*, *52*(3), 425-436. https://doi.org/10.1016/j.neuron.2006.08.028

Mathejczyk, T. F., & Wernet, M. F. (2019). Heading choices of flying Drosophila under changing angles of polarized light. *Sci Rep*, *9*(1), 16773. https://doi.org/10.1038/s41598-019-53330-y

Mathejczyk, T. F., & Wernet, M. F. (2020). Modular assays for the quantitative study of visually guided navigation in both flying and walking flies. *Journal of Neuroscience Methods*, *340*, 108747. https://doi.org/https://doi.org/10.1016/j.jneumeth.2020.108747

Mather, J., & Anderson, R. C. (1993). Personalities of octopuses (Octopus rubescens). *Journal of Comparative Psychology*, *107*, 336-340.

Mischel, W. (1968). *Personality and assessment*. Wiley.

Mischel, W. (1973). Toward a cognitive social learning reconceptualization of personality. *Psychological Review*, *80 4*, 252-283.

Mischel, W., & Shoda, Y. (1995). A cognitive-affective system theory of personality: reconceptualizing situations, dispositions, dynamics, and invariance in personality structure. *Psychological Review*, *102*(2), 246-268. https://doi.org/10.1037/0033-295x.102.2.246

Mischel, W., & Shoda, Y. (1998). RECONCILING PROCESSING DYNAMICS AND PERSONALITY DISPOSITIONS. *Annual Review of Psychology*, *49*(1), 229-258. https://doi.org/10.1146/annurev.psych.49.1.229

Mowles, S. L., Cotton, P. A., & Briffa, M. (2012). Consistent crustaceans: the identification of stable behavioural syndromes in hermit crabs. *Behavioral Ecology and Sociobiology*, *66*(7), 1087-1094. https://doi.org/10.1007/s00265-012-1359-7

Neuser, K., Triphan, T., Mronz, M., Poeck, B., & Strauss, R. (2008). Analysis of a spatial orientation memory in Drosophila. *Nature*, *453*(7199), 1244-1247. https://doi.org/10.1038/nature07003

Otsuna, H., & Ito, K. (2006). Systematic analysis of the visual projection neurons of Drosophila melanogaster. I. Lobula-specific pathways. *J Comp Neurol*, *497*(6), 928-958. https://doi.org/10.1002/cne.21015

Pantoja, C., Hoagland, A., Carroll, E. C., Karalis, V., Conner, A., & Isacoff, E. Y. (2016). Neuromodulatory Regulation of Behavioral Individuality in Zebrafish. *Neuron*, *91*(3), 587-601. https://doi.org/10.1016/j.neuron.2016.06.016

Partridge, L. (1976). Individual differences in feeding efficiencies and feeding preferences of captive great tits. *Animal Behaviour*, *24*(1), 230-240. https://doi.org/https://doi.org/10.1016/S0003-3472(76)80119-4

Pfeiffer, B. D., Ngo, T. T., Hibbard, K. L., Murphy, C., Jenett, A., Truman, J. W., & Rubin, G. M. (2010). Refinement of tools for targeted gene expression in Drosophila. *Genetics*, *186*(2), 735-755. https://doi.org/10.1534/genetics.110.119917

Pulver, S. R., Pashkovski, S. L., Hornstein, N. J., Garrity, P. A., & Griffith, L. C. (2009). Temporal dynamics of neuronal activation by Channelrhodopsin-2 and TRPA1 determine behavioral output in Drosophila larvae. *J Neurophysiol*, *101*(6), 3075-3088. https://doi.org/10.1152/jn.00071.2009

Quinn, W. G., Harris, W. A., & Benzer, S. (1974). Conditioned Behavior in Drosophila melanogaster. *Proceedings of the National Academy of Sciences*, *71*(3), 708-712. https://doi.org/10.1073/pnas.71.3.708

Reale, D., Reader, S. M., Sol, D., McDougall, P. T., & Dingemanse, N. J. (2007). Integrating animal temperament within ecology and evolution. *Biol Rev Camb Philos Soc*, *82*(2), 291-318. https://doi.org/10.1111/j.1469-185X.2007.00010.x

Robie, A. A., Hirokawa, J., Edwards, A. W., Umayam, L. A., Lee, A., Phillips, M. L., Card, G. M., Korff, W., Rubin, G. M., Simpson, J. H., Reiser, M. B., & Branson, K. (2017). Mapping the Neural Substrates of Behavior. *Cell*, *170*(2), 393-406 e328. https://doi.org/10.1016/j.cell.2017.06.032

Ross, L. (1977). The Intuitive Psychologist And His Shortcomings: Distortions in the Attribution Process11The author gratefully acknowledges the assistance of Teresa Amabile, Daryl Bern, Phoebe Ellsworth, Baruch Fischhoff, David Greene, Larry Gross, Mark Lepper, Richard Nisbett, Julia Steinmetz, Amos Tversky, and Philip Zimbardo, all of whom have contributed useful

comments and suggestions concerning both the manuscript and the research and conceptual analysis it reports. The preparation of this chapter and reported research were supported by National Institute of Mental Health Research Grant MH 24134. In L. Berkowitz (Ed.), *Advances in Experimental Social Psychology* (Vol. 10, pp. 173-220). Academic Press. https://doi.org/https://doi.org/10.1016/S0065-2601(08)60357-3

Schuett, W., Dall, S. R. X., Baeumer, J., Kloesener, M. H., Nakagawa, S., Beinlich, F., & Eggers, T. (2011). Personality variation in a clonal insect: The pea aphid, Acyrthosiphon pisum. *Developmental Psychobiology*, *53*(6), 631-640. https://doi.org/https://doi.org/10.1002/dev.20538

Seelig, J. D., Chiappe, M. E., Lott, G. K., Dutta, A., Osborne, J. E., Reiser, M. B., & Jayaraman, V. (2010). Two-photon calcium imaging from head-fixed Drosophila during optomotor walking behavior. *Nat Methods*, *7*(7), 535-540. https://doi.org/10.1038/nmeth.1468

Sih, A., Cote, J., Evans, M., Fogarty, S., & Pruitt, J. (2012). Ecological implications of behavioural syndromes. *Ecology Letters*, *15*(3), 278-289. https://doi.org/https://doi.org/10.1111/j.1461-0248.2011.01731.x

Spoolder, H. A. M., Burbidge, J. A., Lawrence, A. B., Simmins, P. H., & Edwards, S. A. (1996). Individual behavioural differences in pigs: Intra- and inter-test consistency. *Applied Animal Behaviour Science*, *49*(2), 185-198. https://doi.org/10.1016/0168-1591(96)01033-7

Strauss, R., Hanesch, U., Kinkelin, M., Wolf, R., & Heisenberg, M. (1992). No-Bridge of Drosophila Melanogaster: Portrait of a Structural Brain Mutant of the Central Complex. *Journal of Neurogenetics*, *8*(3), 125-155. https://doi.org/10.3109/01677069209083444

Strauss, R., Renner, M., & Götz, K. (2001). Task-specific association of photoreceptor systems and steering parameters in Drosophila. *Journal of Comparative Physiology A*, *187*(8), 617-632. https://doi.org/10.1007/s003590100234

Sweeney, S. T., Broadie, K., Keane, J., Niemann, H., & O'Kane, C. J. (1995). Targeted expression of tetanus toxin light chain in Drosophila specifically eliminates synaptic transmission and causes behavioral defects. *Neuron*, *14*(2), 341-351. https://doi.org/10.1016/0896-6273(95)90290-2

Takola, E., & Schielzeth, H. (2022). Hutchinson's ecological niche for individuals. *Biology & Philosophy*, *37*(4), 25. https://doi.org/10.1007/s10539-022-09849-y

Traynor, B. J., & Singleton, A. B. (2010). Nature versus Nurture: Death of a Dogma, and the Road Ahead. *Neuron*, *68*(2), 196-200. https://doi.org/https://doi.org/10.1016/j.neuron.2010.10.002

Valente, D., Golani, I., & Mitra, P. P. (2007). Analysis of the trajectory of Drosophila melanogaster in a circular open field arena. *PLoS One*, *2*(10), e1083. https://doi.org/10.1371/journal.pone.0001083

Vansteelandt, K., & Van Mechelen, I. (2004). The personality triad in balance: Multidimensional individual differences in situation–behavior profiles. *Journal of Research in Personality*, *38*(4), 367-393. https://doi.org/https://doi.org/10.1016/j.jrp.2003.08.001

Versace, E., Caffini, M., Werkhoven, Z., & de Bivort, B. L. (2020). Individual, but not population asymmetries, are modulated by social environment and genotype in Drosophila melanogaster. *Scientific Reports*, *10*(1), 4480. https://doi.org/10.1038/s41598-020-61410-7

Warren, T. L., Weir, P. T., & Dickinson, M. H. (2018). Flying Drosophila melanogaster maintain arbitrary but stable headings relative to the angle of polarized light. *J Exp Biol*, *221*(Pt 9). https://doi.org/10.1242/jeb.177550

Weisbuch, M., Slepian, M. L., Clarke, A., Ambady, N., & Veenstra-Vanderweele, J. (2010). Behavioral Stability Across Time and Situations: Nonverbal Versus Verbal Consistency. *J Nonverbal Behav*, *34*(1), 43. https://doi.org/10.1007/s10919-009-0079-9

Werkhoven, Z., Bravin, A., Skutt-Kakaria, K., Reimers, P., Pallares, L. F., Ayroles, J., & de Bivort, B. L. (2021). The structure of behavioral variation within a genotype. *Elife*, *10*, e64988. https://doi.org/10.7554/eLife.64988

Werkhoven, Z., Rohrsen, C., Qin, C., Brembs, B., & de Bivort, B. (2019). MARGO (Massively Automated Real-time GUI for Object-tracking), a platform for high-throughput ethology. *PLoS One*, *14*(11), e0224243. https://doi.org/10.1371/journal.pone.0224243

Xu, C. S., Januszewski, M., Lu, Z., Takemura, S.-y., Hayworth, K. J., Huang, G., Shinomiya, K., Maitin-Shepard, J., Ackerman, D., Berg, S., Blakely, T., Bogovic, J., Clements, J., Dolafi, T., Hubbard, P., Kainmueller, D., Katz, W., Kawase, T., Khairy, K. A.,…Plaza, S. M. (2020). A Connectome of the Adult Drosophila Central Brain. *bioRxiv*, 2020.2001.2021.911859. https://doi.org/10.1101/2020.01.21.911859

Zheng, Z., Lauritzen, J. S., Perlman, E., Robinson, C. G., Nichols, M., Milkie, D., Torrens, O., Price, J., Fisher, C. B., Sharifi, N., Calle-Schuler, S. A., Kmecova, L., Ali, I. J., Karsh, B., Trautman, E. T., Bogovic, J. A., Hanslovsky, P., Jefferis, G., Kazhdan, M.,…Bock, D. D. (2018). A Complete Electron Microscopy Volume of the Brain of Adult Drosophila melanogaster. *Cell*, *174*(3), 730-743 e722. https://doi.org/10.1016/j.cell.2018.06.019